이학박사 학위논문

The role of dynactin1 in osteoclastogenesis

파골세포 분화에 대한 dynactin1의 역할

2016년 2월

서울대학교 대학원
치의과학과 세포및발생생물학 전공
이 용 덕

The role of dynactin1 in osteoclastogenesis

by

Yong Deok Lee

Advisor:

Prof. Hong-Hee Kim, Ph.D

A Thesis Submitted in Partial Fulfillment of the
Requirements for the Degree of Doctor of Philosophy

February, 2016

Division of Cell and Developmental Biology
Department of Dental Science, School of Dentistry
Seoul National University

Abstract

The role of dynactin1 in osteoclastogenesis

Yong Deok Lee

Department of Cell and Developmental Biology

The Graduate School

Seoul National University

(Directed by Prof. Hong-Hee Kim, Ph.D)

Bone remodeling is regulated by bone forming osteoblasts and bone-resorbing osteoclasts. The imbalance between osteoblasts and osteoclasts activities leads to bone related diseases. Osteoclast is differentiated from hematopoietic stem cell-derived precursor cells by M-CSF and RANKL. Microtubule motor cytoplasmic dynein and its adaptor dynactin have been shown to function in diverse processes including vesicular transport, mitotic spindle formation, and cytokinesis. Dynactin, named as a dynein activator, is important for the dynein's function. Dynactin is a giant multi-subunit complex, which

consists of 11 different subunits, and its molecular weight reaches 1 mDa. Binding dynactin to dynein is required for cytoplasmic dynein-driven activities. Its binding to dynein helps the enhancement of dynein's processivity and targets dynein to particular cellular location. Dynactin1 (DCTN1), ubiquitously expressed in eukaryotes, is the largest subunit pivotal for dynactin function. DCTN1 can concurrently bind to both microtubules and dynein, and thereby regulates dynein's processivity. The mutated DCTN1 (G59S) protein, which lacks the ability to bind to microtubules, is associated with development of neurodegenerative disorders.

Here I show that DCTN1 has an important role in osteoclast differentiation. Among the six dynactin gene family members, the DCTN1 mRNA was highly expressed in osteoclast precursor cells. The expression level of DCTN1 was increased at early stage by RANKL and the elevated level was maintained during osteoclastogenesis. Knockdown of DCTN1 decreased RANKL-induced osteoclast differentiation and suppressed the ERK1/2, p38, JNK, and Akt signaling pathways. The induction of NFATc1 and c-Fos, important osteoclastogenic transcription factors, was also inhibited by DCTN1 silencing. Moreover, DCTN1 knockdown significantly reduced bone resorption activity and disrupted the formation of actin-ring. The decrease in both NFATc1 and c-Fos by DCTN1 silencing could be attributed to the inhibition of RANKL-

dependent Cdc42/PAK2 signaling pathway. Silencing of PAK2, an effector molecule of Cdc42 signaling, inhibited osteoclastogenesis and NFATc1 induction. DCTN1 siRNA injection onto mice calvariae disrupted bone resorption and OC formation by RANKL. Forced expression of constitutively active Cdc42 in DCTN1-silenced bone marrow-derived macrophages rescued osteoclast differentiation. The expression of NFATc1 and c-Fos was also recovered. Interestingly, the overexpression of DCTN1 also reduced osteoclast differentiation. These results suggest that abnormal levels of DCTN1 interfere with normal osteoclastogenesis. Taken together, DCTN1 has a critical role in osteoclastogenesis.

Keywords : Osteoclast differentiation, dynactin1, NFATc1, c-Fos, Cdc42, PAK

Student Number: 2009-23600

CONTENTS

LIST OF FIGURES

LIST OF TABLES

ABBREVIATIONS

M-CSF	Macrophage-colony stimulating factor
RANK	Receptor activator of nuclear factor κB (NF-κB)
RANKL	Receptor activator of nuclear factor κB (NF-κB) ligand
BMMs	Bone marrow-derived macrophages
MNCs	Multinucleated cells
HSCs	Hematopoietic stem cells
MSCs	Mesenchymal stem cells
μ-CT	Micro-computed tomography
NFATc1	Nuclear factor of activated T cell c1
TRAP	Tartrate-resistant acid phosphatase
Ctsk	Cathepsin K
MAPK	Mitogen-activated protein kinase
ERK	Extracellular signal-regulated kinase
JNK	c-Jun N-terminal kinase
STAT3	Signal transducer and activator of transcription 3
Cdc42	Cell division control protein 42
Rac1	Ras-related C3 botulinum toxin substrate 1

Arp1	Actin-related protein 1
Arp11	Actin-related protein 11
CapZα	Capping protein muscle Z-line, alpha
CapZβ	Capping protein muscle Z-line, beta

I. Introduction

I.1. Bone remodeling

Maintenance of bone mass requires continuous reconstruction that is mediated by osteoclasts (OCs) and osteoblasts (OBs) (Nicholls et al., 2012) (Fig. 1). OCs, the bone-resorbing cells of hematopoietic stem cell origin, contribute to bone homeostasis by removing old bones. Mature OCs reorganize the actin cytoskeleton into the actin-ring structure and attach to the bone surface, and this attachment structure of the OC membrane to bone surface is called sealing-zone. In this phase, OCs secrete protons and lysosomal enzymes, required for bone degradation, into the lacuna (Takahashi et al., 2007; Teitelbaum, 2000). The disruption of OC differentiation or its function leads to several bone-related diseases (Kong et al., 1999; Mundy, 2002; Teitelbaum, 2000). Therefore, understanding the mechanism by which OC differentiation is regulated is critical to develop the therapeutic strategies for bone-related diseases.

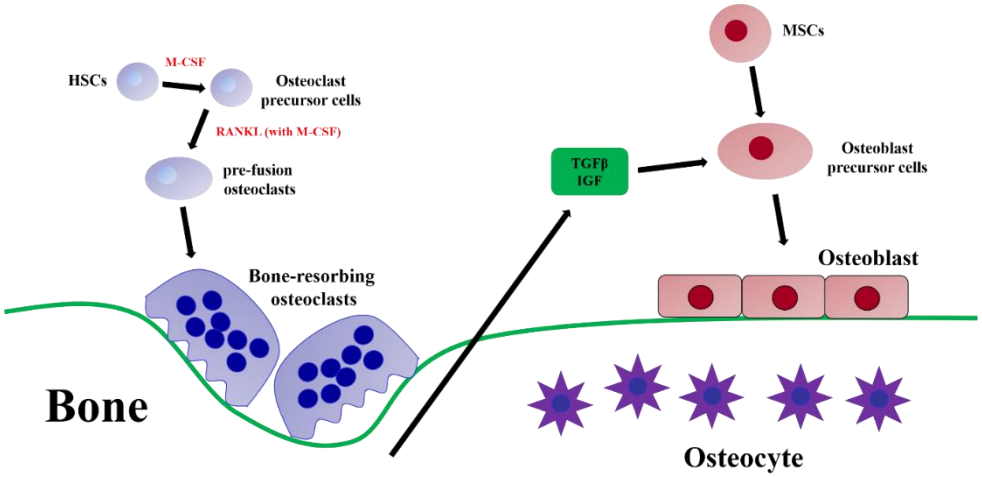

Modified from Nature Reviews Cancer | Vol. 11 | June 2011

Figure 1. The coupling of OCs and OBs during bone remodeling.

Bone is continuously reconstituted by the harmony of OCs and OBs to maintain its homeostasis. Hematopoietic stem cell (HSC)-derived OC precursor cells differentiate into mature OCs by M-CSF and RANKL. Then, activated OCs resorb mineralized bone surface. OB precursor cells originated from mesenchymal stem cells (MSCs) are recruited at the resorbed bone surface and differentiate into mature OBs, which replace old bone with new bone. OBs maturate into osteocytes that are embedded in mineralized bone. Osteocytes participate in bone remodeling by sensing mechanical strain and regulating OCs and OBs.

I.2. Osteoclast differentiation

OCs, a specialized bone-resorbing cell arising from monocytes/macrophages (Fig. 2), have an essential role in bone remodeling (Boyle et al., 2003). OCs bind to bone surface and resorb the mineralized bone by secretion of protons and lysosomal proteolytic enzymes into lacuna (Boyle et al., 2003; Georgess et al., 2014). OC precursors undergoes sequential steps for the differentiation (proliferation, fusion, maturation) which is regulated by macrophage-colony stimulating factor (M-CSF) and receptor activator of nuclear factor-κB ligand (RANKL) (Takayanagi, 2005). M-CSF supports survival and proliferation during osteoclastogenesis, while RANKL promotes the maturation of OC precursor cells into multinucleated cells (Negishi-Koga and Takayanagi, 2009).

Interaction of RANKL with RANK induces signal transduction required for osteoclastogenesis (Fig. 3). The recruitment of tumor necrosis factor receptor–associated factors 6 (TRAF6) activates mitogen-activated protein kinases (MAPKs) signaling cascades involving extracellular-signal-regulated kinases (ERK), c-Jun N-terminal kinases (JNK), and p38, also phosphatidylinositol 3-kinase (PI3K)/Akt pathways (Lee and Kim, 2003; Takayanagi, 2005). RANKL also activates activator protein-1 (AP-1) transcription factor complex through an induction of its crucial component c-Fos in an early phase during osteoclastogenesis (Grigoriadis et al., 1994). The induction of c-Fos was

promoted by Ca^{2+}⁄calmodulin-dependent protein kinases (CaMKs) and cyclic AMP-responsive element-binding protein (CREB) (Sato et al., 2006). Ultimately, these signaling cascades trigger the expression of nuclear factor of activated T cell cytoplasmic 1 (NFATc1), a master transcription factor for OC differentiation (Takayanagi et al., 2002). NFAT family members are regulated by calcineurin, which is activated by Ca^{2+}-dependent manner (Guerini, 1997; Hogan et al., 2003; Klee et al., 1998). The dephosphorylation of serine residues in NFATc1 by calcineurin triggers its translocation into the nucleus upon RANKL stimulation. NFATc1 expression is further enhanced by an autoamplification mechanism via binding of NFATc1 on its own promoter (Negishi-Koga and Takayanagi, 2009; Takayanagi et al., 2002). NFATc1, interacting with its binding partners MITF and PU.1, induces the expression of tartrate resistant acid phosphatase (TRAP), matrix metalloproteinases (MMPs), and cathepsin K (Ctsk), which are required for the osteoclastic resorption (Nakashima and Takayanagi, 2011; Song et al., 2009).

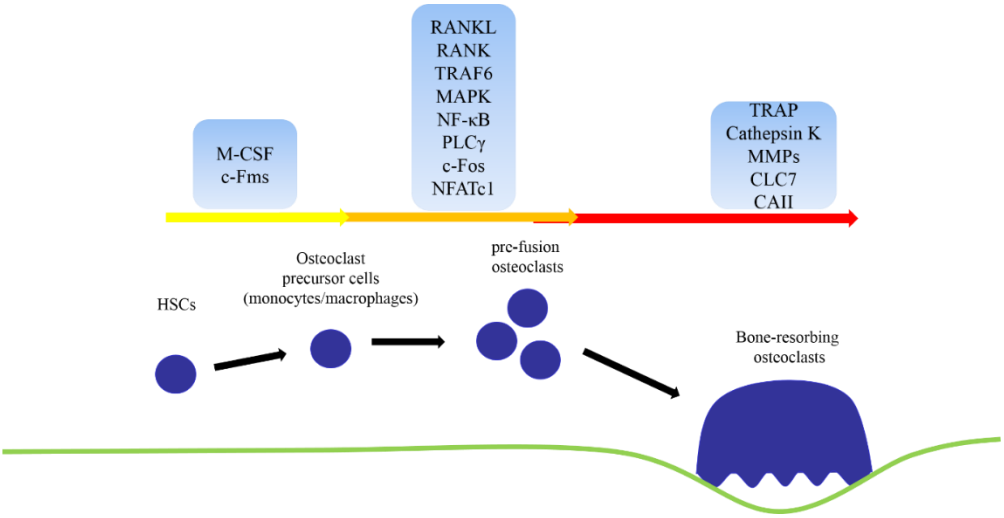

Modified from Immunological Review | Vol. 231 | September 2009

Figure 2. The differentiation of OCs from hematopoietic stem cells.

HSCs differentiate into OC precursor cells by M-CSF. M-CSF increases cell proliferation and induces the RANK expression in OC precursor cells, thereby enhances response to its ligand RANKL. The OC precursor cells undergo cell-cell fusion which is activated by RANKL-induced downstream signaling molecules such as TRAF6, PLCγ2, c-Fos, NFATc1, DC-STAMP. In the maturation stage, OCs express diverse molecules important for resorbing activity such as chloride channel 7 (CLC7), osteopetrosis associated transmembrane protein 1 (OSTM1), carbonic anhydrase II (CAII), Ctsk, and TRAP.

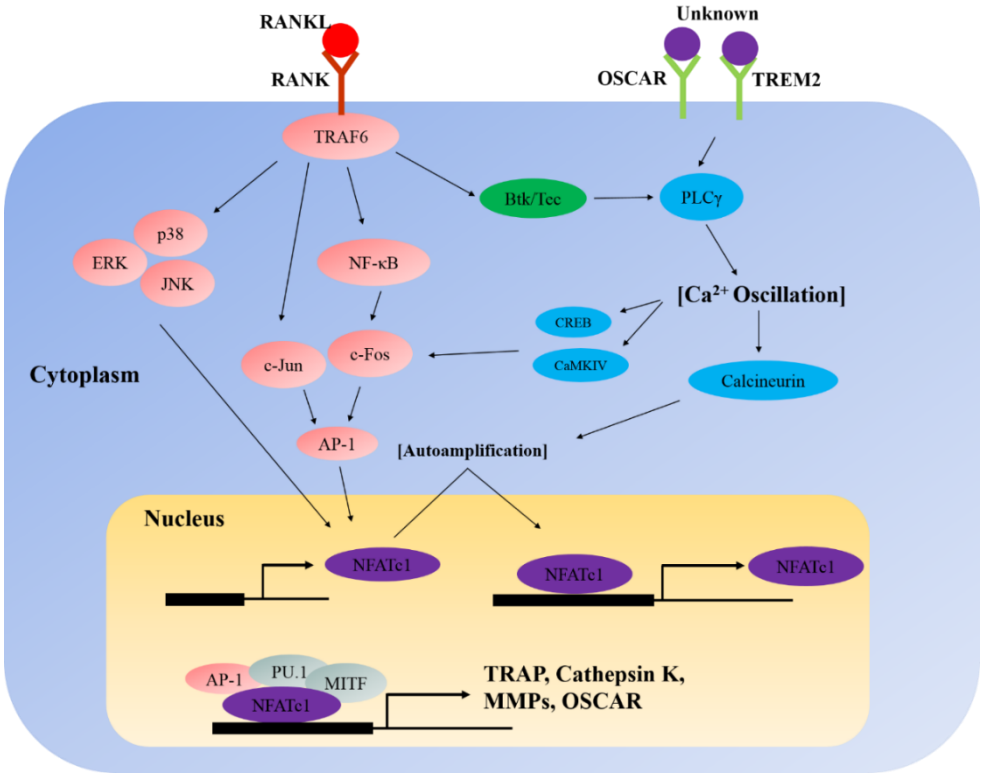

Modified from Arthritis Research & Therapy | Vol. 219 | May 2011

Figure 3. RANKL-induced signaling cascades during OC differentiation.

RANKL-RANK binding results in the recruitment of TRAF6, which activates MAPKs, such as ERK1/2, p38, and JNK. RANKL also stimulates the induction of c-Fos through NF-κB, CaMKIV and CREB. These signaling pathways are important for the NFATc1 expression, a master transcription factor for osteoclastogenesis. RANK signaling cooperates with phospholipase Cγ (PLCγ)

and activate calcium signaling, which is important for the autoamplification of NFATc1. NFATc1, in cooperation with AP-1, MITF and PU.1, promotes the induction of TRAP, MMPs, Ctsk, and OSCAR, which are important for OC functions.

I.3. Dynactin

Dynein, first identified as a high molecular weight microtubule-based motor, consists of heavy chains, intermediate chains, and light chains. Dynein transports diverse cellular cargos such as proteins, vesicles, and organelles (Kardon and Vale, 2009; Paschal et al., 1987). Dynactin is an indispensable component of the dynein complex (Fig. 4). It is an important adaptor protein of the microtubule motor. Dynactin itself is a large complex which comprises 11 different subunits, $p150^{Glued}$ (DCTN1), p50 (DCTN2), p24 (DCTN3), p62 (DCTN4), p25 (DCTN5), p27 (DCTN6), Arp1/11, actin, and actin capping protein α and β subunits (Kardon and Vale, 2009). It has been reported that dynactin has an essential role for almost all cellular functions of dynein (Karki and Holzbaur, 1999; Schroer, 2004). Dynactin helps interaction between dynein and its cargos, enhances dynein processivity and translocates dynein to particular cellular locations (Kardon and Vale, 2009). Among the 11 subunits, DCTN1 is the largest and most important subunit. DCTN1 increased dynein activity (Kardon and Vale, 2009; Schroer, 2004). The N-terminus of DCTN1 (aa 1–110) contains a conserved CAP-Gly (cytoskeleton-associated protein, glycine-rich) motif which has been shown to interact with microtubules (Waterman-Storer et al., 1995). The interaction of CAP-Gly motif with microtubules is essential for its ability to increase the processivity of the dynein motor. Moreover, it has been reported that

DCTN1 interacts with its binding partner such as EB1, CLIP-170, and microtubule-binding proteins through CAP-Gly domain. (Schroer, 2004).

DCTN1 has been implicated in diverse cellular events, such as transport of cellular components, mitosis, cytokinesis, and autophagy (Ikenaka et al., 2013; Karki and Holzbaur, 1999; Vallee et al., 2004). Direct interaction of DCTN1 with the intermediate chain of dynein has been considered to be the crucial step for dynein-mediated organelle transport (Kardon and Vale, 2009; Waterman-Storer et al., 1997). DCTN1 directly interacts with the Hermansky-Pudlak syndrome 6 protein (HPS6) to regulate the transport of lysosomes to the perinuclear region and regulates lysosomal degradation of endocytosed cargos (Li et al., 2014). Dynein/dynactin complex has an essential role in chromosome movements, spindle formation, and checkpoint silencing during mitosis (Howell et al., 2001; Karki and Holzbaur, 1999; Sharp et al., 2000; Varma et al., 2008).

Dynein/Dynactin complex has been implicated in several diseases. The functional disruption of dynactin complex causes neurodegenerative diseases, including Alzheimer's disease, amyotrophic lateral sclerosis (ALS), Parkinson's disease, and atypical Parkinsonian syndromes (De Vos et al., 2008; Stockmann et al., 2013). The disruption of axonal transport is linked with almost all motor protein-related diseases. The G59S missense mutation in the CAP-Gly motif of DCTN1 inhibits the binding of dynactin to microtubules and increase the

aggregation of dynactin. The disruption of the interaction inhibits axonal transport (Waterman-Storer et al., 1997). The G59S mutation in DCTN1 elevated cytosolic aggregates of dynactin complex (Levy et al., 2006). In patients with motor neuron disease, the accumulation of both dynein and dynactin in perinuclear aggregates has been observed (Levy and Holzbaur, 2006). Therefore, mutation in the gene encoding DCTN1 can disrupt normal neuronal function. Cancers are characterized by excessive proliferation and, therefore, molecules involved in cell division can be effective anticancer therapeutic targets. The motor protein or its associated proteins may be considered to be one of the anticancer therapy targets (Kunoh et al., 2010; Rodriguez-Gonzalez et al., 2008). In a recent study, DCTN1, with the end binding 1 (EB1) and Clasp1, was shown to be required for human endothelial cells tube formation inducing microtubule assembly and asymmetric cytoskeletal polarization, and to modulate signal transduction by activating Pak, Raf, and ERK kinases (Kim et al., 2013a).

The small GTPases act as molecular switches, by cycling between GTP-bound form (active) and GDP-bound form (inactive), they have diverse roles in cellular function (Jaffe and Hall, 2005). Cdc42, a small GTPase, was first identified as an essential gene product in *Saccharomyces cerevisiae* involved in actin cytoskeletal regulation (Johnson and Pringle, 1990). Cdc42 has been implicated in cytoskeleton organization, transcription, cell cycle progression,

vesicle trafficking, survival, and other cell functions (Melendez et al., 2011). Cdc42 also implicated in dynein/dynactin-mediated cytoskeleton regulation. In a previous report, Lysophosphatidic acid (LPA) promotes dynein/dynactin-mediated microtubule-organizing center reorientation (MTOC) during migration of fibroblasts (Palazzo et al., 2001). In this report, LPA increased GTP-bound Cdc42. The overexpression of dominant- negative Cdc42 in NIH3T3 cells sufficiently inhibited MTOC reorientation. The disruption of dynein/dynactin function with blocking antibody for dynein also inhibited LPA-mediated MTCO regulation. These results indicate that Cdc42 can be associated with dynein/dynactin complex to regulate cellular events.

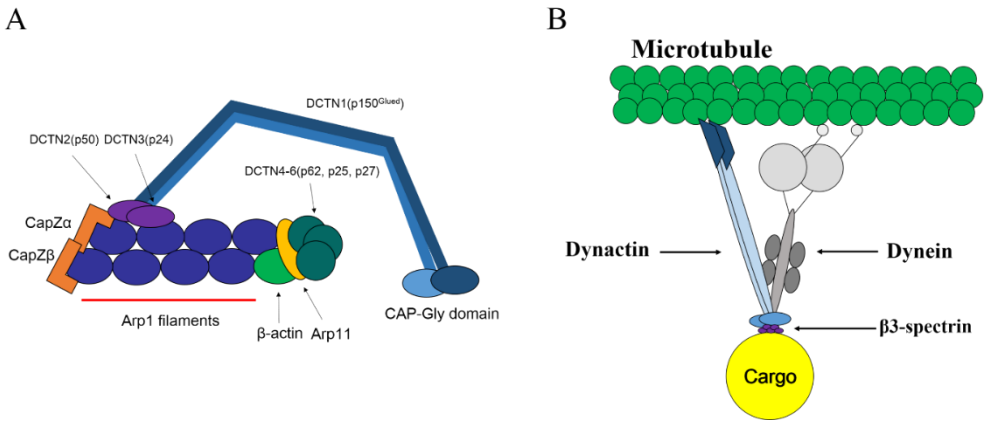

Modified from Pharmacology & Therapeutics | Vol. 130 | June 2011

Figure 4. Schematic representation of dynein–dynactin structure.

(A) Dynactin is an adaptor protein complex for dynein which enhances dynein processivity. It consists of 11 subunits, including p150Glued (DCTN1), p50 (DCTN2), p24 (DCTN3), p62 (DCTN4), p25 (DCTN5), p27 (DCTN6), Arp1/11, and capping proteins. Arp1 forms short filament which is an important scaffold of dynactin complex. One end of Arp filament terminated with the capping protein, CapZα and β. The opposite end is endorsed by Arp11 and DCTN4-6. DCTN1 interacts with Arp1 filament through the docking site which is made of DCTN2 and 3. (B) Dynein/dynactin drives cargoes along microtubules from minus ends to plus ends. β3-Spectrin mediates binding of cargoes to dynein/dynactin.

I.4. Purpose of the study

In a previous report, overexpressed DCTN2, a subunit of dynactin complex, disrupted OC differentiation and Ctsk secretion (Ng et al., 2013). However, the roles of other subunits are unclear. In this study, I focused on DCTN1, the most important subunit of dynactin complex. I examined whether DCTN1 is involved in regulation of osteoclastogenesis via loss- and gain-of-function approaches.

II. Materials and Methods

II.1. Animal

5-week-old ICR mice for preparation of primary bone marrow derived-macrophages (BMMs) were purchased from OrientBio (Seongnam, Korea). All mice were fed a regular diet and water and maintained in a 12 hr light/night cycle at the animal facility of Seoul National University School of Dentistry. All animal experiments were performed with the approval of the Institutional Animal Care and Use Committee at Seoul National University.

II.2. Reagents and antibodies

Anti-NFATc1, anti-c-Fos, anti-Cdc42, and anti-DCTN1 were purchased from Santa Cruz Biotechnology (Paso Robles, CA, USA). Anti-phospo-PAK1 was purchased from Cell Signaling Technology (Beveryly, MA, USA). Anti-phospho-PAK2 was purchased from GeneTex (Irvine, CA, USA). Anti-phospho-PAK4 was purchased from Bioss Antibodies (Woburn, MA, USA). All other antibodies were purchased from Cell Signaling Technology. HiPerFect was purchased from QIAGEN (Hilden, Germany). Human soluble RANKL and M-CSF were purchased from Pepro-Tech (Rocky Hill, NJ, USA). Cell counting kit-

8 (CCK) was obtained from Dojindo (Kumamoto, Japan).

II.3. Bone marrow-derived macrophage (BMM) preparation

Bone marrow of tibiae and femurs of 5-week-old female mice was flushed with α-MEM (Welgene, Daegu, Korea). After removing erythrocytes with hypotonic buffer, cells were cultured in α-MEM containing 10% FBS for 24 hr. Then, non-adherent cells were further cultured on petri-dishes in α-MEM containing 10% FBS and 1% antibiotics (10,000 units/ml of penicillin and 10 mg/ml of streptomycin) and with M-CSF (30 ng/ml) for 3 days. Non-adherent cells were washed out. Adherent cells at this stage were considered BMMs.

II.4. Osteoclast differentiation and TRAP staining

For osteoclast differentiation, BMMs (3×10^4 cells/well in 48-well plates) were cultured with M-CSF (30 ng/ml) and RANKL (200 ng/ml) in α-MEM containing 10% FBS and 1% antibiotics (10,000 units/ml of penicillin and 10 mg/ml of streptomycin) for 4 days. The culture medium was changed at day 2. TRAP-positive multinucleated cells (MNCs) were observed at day 4. The cells were fixed with 3.7% formaldehyde for 20 min at room temperature and permeabilized

with 0.1% Triton X-100 for 5 min. After being washed twice with PBS, the cells were stained using a Leukocyte Acid Phosphatase Assay Kit from Sigma (St. Louis, MO, USA) according to the manufacturer's instructions. After staining, cells were washed with distilled water and observed under a light microscope. TRAP-positive cells containing more than three nuclei were considered to be differentiated osteoclasts.

II.5. Small interfering RNA (siRNA) transfection

Target gene-specific siRNA oligonucleotides were purchased from Invitrogen (Carlsbad, CA, USA). BMMs were transfected with siRNA (40 nM) using HiPerFect (QIAGEN) following the manufacturer's instruction. Briefly, 3×10^5 cells were seeded in 6-well culture plates and incubated for 24 hr in the presensce of M-CSF (30 ng/ml). Mixtures of 40 nM of siRNA, HiPerFect reagent and medium were prepared prior to transfection. In this step, the medium without any serum and antibiotics was used. Solutions were mixed gently and incubated for 10 minutes at room temperature to allow the formation of transfection complexes. 100 μl of transfection mixture was added to the plates and incubated for 24 hr at 37℃.

II.6. Real-time PCR

Total RNA was isolated using TRIzol reagent (Invitrogen). Then, cDNA synthesis was performed with 3 μg of total RNA using Superscript II reverse transcriptase (Invitrogen) according to the manufacturer's instructions. To analyze gene expression, cDNA was amplified with SYBR Green Master Mix reagents (Kapa Biosystems, MA, USA) using an ABI 7500 instrument (Applied Biosystems, Carlsbad ,CA, USA). The detector was programmed with the following PCR conditions: 40 cycles for 3 sec denaturation at 95℃ and 33 sec amplification at 60℃. All reactions were run in triplicates and were normalized using the β-actin level. The mRNA expression level was calculated using the $2^{-\Delta\Delta CT}$ method. All primer sets for RT-PCR and real-time PCR were listed in Table 1.

II.7. Retroviral DNA transduction

pcDNA3-EGFP-Cdc42 Q61L (constitutive active form) was kindly provided by Eun-Ju Chang (University of Ulsan College of Medicine, Seoul, Republic of Korea) and pcDNA3-DCTN1 was kindly provided by Stefan Liebau (Department of Neurology, Ulm University, Ulm, Germany). Each plasmid was subcloned into pMX vector. For retroviral packaging, Plat-E cells were transfected with

pMX-Cdc42 Q61L or pMX-DCTN1 and cultured for 2 days. The culture medium containing retroviruses was collected and filtered with 0.45 μm syringe filter (Satorius, Göttingen, Germany). BMMs were infected with retrovirus-containing supernatant using 10 μg/ml hexadimethrine bromide (Polybrene; Sigma) for 24 hr.

II.8. Western blotting

Whole cell extracts were prepared by lysing cells with RIPA buffer [50 mM Tris-HCl, pH 8.0, 150 mM NaCl, 1% NP-40, 0.5% sodium deoxycholate, 0.1% SDS, 0.5 mM PMSF, proteinase inhibitor cocktail (Roche, Mannheim, Germany), 100 mM sodium vanadate, and 0.5 M sodium fluoride] and centrifuged at 14,000 rpm for 20 min at 4℃. After protein quantification, cell extracts were separated on polyacrylamide gels and transferred onto nitrocellulose membranes. After blocking for 1 hr with 5% skim milk in Tris-buffered saline containing 0.1% Tween 20, the membranes were incubated overnight at 4℃ with the primary antibody. The next day, the membranes were incubated with the horseradish peroxidase-conjugated secondary antibody, and developed using an enhanced chemiluminescence reagents.

II.9. Cell viability assay

BMMs transfected with DCTN1 siRNA were cultured in the presence of M-CSF (30 ng/ml) and RANKL (200 ng/ml). For CCK assay, cells were incubated with 10% CCK solution in cell culture medium for 1 hr at 37℃. After incubation, optical density was measured with an ELISA reader (iMARK Microplated Absorbance Reader, Bio-Rad, Hercules, CA, USA) at 450 nm.

II.10. Terminal deoxynucleotidyl transferase dUTP nick end labeling (TUNEL) assay

BMMs transfected with control or DCTN1 siRNA were incubated with M-CSF (30 ng/ml) and RANKL (200 ng/ml) for 2 days. TUNEL assays were performed using an In Situ Cell Death Detection Kit (Roche) according to the manufacturer's instructions. Briefly, cells were fixed with 3.7% formaldehyde for 1 hr at room temperature and permeabilized with 0.1% Triton X-100 for 2 min on ice. Cells were rinsed with PBS and subsequently incubated with 50 μl lable solution in a humidified atmosphere for 60 min at 37℃. Cells were observed by Zeiss LSM 5 PASCAL laser-scanning microscope (Carl Zeiss Microimaging GmbH, Goettingen, Germany) with an excitation wavelength in the 450 nm.

II.11. In vitro resorption assay

BMMs were seeded on dentin slices (Immunodiagnostic Systems Inc, Boldon, United Kingdom). Next day, cells were transfected with siRNA and further cultured in the presence of M-CSF (30 ng/ml) and RANKL (200 ng/ml) for 9 days. Typically 3 dentin slices per group were used. Cells were removed with 5% sodium hypochlorite for 10 min. Dentin slices were wiped using a cotton swab and rinsed with distilled water. After removing cells, resorption pits were assessed and the area and depth of resorption pits were measured by Zeiss LSM 5 PASCAL laser-scanning microscope.

II.12. Confocal microscopy

BMMs were seeded on glass cover slips in 24-well plates at a density of 5×10^4 cells per well. Cultured cells were fixed with 3.7% formaldehyde and permeabilized with 0.1% Triton X-100. Fixed cells were blocked with 1% BSA in PBS, incubated with primary antibody (1:100) at 4℃ overnight and washed with PBS. Cells were then incubated with secondary antibody (1:250) for 2 hr and counterstained with 4′,6-diamidino-2-phenylindole (DAPI). Cells were observed under a Zeiss LSM 5 PASCAL laser-scanning microscope with an X400 objective (CApochromat /1.2 WCorr).

II.13. Actin-ring staining

For actin-ring staining, BMMs transfected with siRNA were cultured on 12 mm round cover glasses in 24 well with M-CSF (30 ng/ml) and RANKL (200 ng/ml) in α-MEM supplemented with 10% FBS for 4 days. Cells were fixed with 3.7% formaldehyde and permeabilized with 0.1% Triton X-100. Then, cells were stained with Alexa Fluor 633-conjugated phalloidin (Invitrogen) for 1 hr at room temperature.

II.14. Active Cdc42 and Rac1 assay

1×10^6 BMM cells were cultured in a 60 mm culture dish. Cells were then transfected with control or DCTN1 siRNA. After 24 hr, cells were serum-starved for 4 hr and stimulated with RANKL (400 ng/ml) for different time periods. For Cdc42 and Rac1 assays, cell lysates were subjected to GST-fusion pull-down using Active Cdc42/Rac1 assay kits (Millipore, Massachusetts, USA) according to the manufacturer's instructions. Briefly, cells were lysed with lysis buffer (125 mM HEPES, pH 7.5, 570 mM NaCl, 5% lgepal CA-630, 50 mM $MgCl_2$, 5 mM EDTA and 10% glycerol) contained in the Active Cdc42/Rac1 Assay kit and incubated with PBD (p21-activated kinase binding domain)-conjugated bead at 4℃ on the rocker. Beads were rinsed 3 times using the lysis buffer. The

precipitated activated forms of Cdc42 and Rac1 were detected by Western blotting.

II.15. In vivo bone resorption assay

Control or DCTN1 siRNA (20 µM; 30 µl) were mixed with Lipofectamine 2000 from Invitrogen (10 µl) and injected onto 5-week-old female mice (n = 5 per group) calvariae 3 times with 2-day intervals. One day after the first injection, collagen sponges soaked in PBS or RANKL (10 µg) were surgically inserted into the center of calvariae. Mice were sacrificed on day 7 and calvariae were collected for TRAP-staining and micro-computed tomography (µCT) analysis (SkyScan, Aartselaar, Belgium; 40 Kv, 250 µA, 7.61 pixel size, threshold maximum 210 and minimum 100).

II.16. Histology and histomorphometry

Mice calvariae (n = 5 per group) were fixed in 4% paraformaldehyde and decalcified in 12% EDTA for 4 weeks. Calvariae were then dehydrated in 70% to 100% ethanol and embedded in paraffin. Tissue sections of 5 µm thickness were used for TRAP staining. Histomorphometric analysis was performed as

described (Chang et al., 2008) using the Osteomeasure program (OsteoMetrics, Inc., Atlanta, GA, USA).

II.17. Immunofluorescence staining on paraffin sections

Paraffin blocks of mice calvariae were sectioned into 5 μm slices using Leica RM2245 microtome (Leica, Buffalo, IL, USA) . The tissue sections were deparaffinized in 100% xylene followed by re-hydration with sequential 100~50% ethanol washes. For immunohistochemical analysis, antigen retrieval was performed by incubation in a citrate buffer (10 mM sodium citrate, 0.05% Tween 20, pH 6.0) at 60℃ for 1 hr. Cells were permeabilized with 0.2% Triton X-100 with gentle agitation for 40 min at room temperature and blocked with 10% BSA in Tris-buffered saline containing 0.1% Tween 20 for 2 hr at room temperature. Then, sectioned slices were incubated with primary antibody (1:100) at 4℃ for overnight and washed with PBS. Cells were then incubated with secondary antibody (1:250) for 2 hr and counterstained with DAPI.

II.18. In vivo apoptosis assay

Apoptotic osteoclasts in calvariae sections were detected by TUNEL-cathepsin K double staining. Briefly, the calvariae sections were stained with cathepsin K

antibody (used as an marker of osteoclasts) after TUNEL staining using an In Situ Cell Death Detection Kit (Roche) according to the manufacturer's instructions. For quantification of apoptotic osteoclasts, 5 representative images were analyzed. The quantitative data were shown as the percentage of TUNEL-positive cells per capthesin K-positive cells.

II.19. Statistical analysis

All in vitro experiments were repeated at least three times. All quantitative experiments were performed at least in triplicate. Student's t test was used to determine the significance between two groups.

Table 1. A list of primer sequences for real-time PCR experiments.

Gene		Sequence	GenBank accession #
		5'- -3'	
DCTN1	Sense	TTGACGTGGGTGGTAGCTGT	NM_007835.2
	Antisense	TCTGCGTCATACTCGCCTTC	
DCTN2	Sense	CAGATGCTGCAATCAACCTT	NM_001190454.1
	Antisense	CAACTTTGGCAGCTTGAGAG	
DCTN2	Sense	CAGTTCATCCTCTCCCAGGT	NM_016890.4
	Antisense	ATACCCTTCCAGGAGAGCCT	
DCTN4	Sense	CACACACAACGGATGAACAA	NM_026302.3
	Antisense	AGGGAAAGTCCAGCAAGTGT	
DCTN5	Sense	ACGTTGGGAAGAACTGTGTG	NM_021608.3
	Antisense	AATCATCAGCTCCTGTGTGC	
DCTN6	Sense	TCAACACCTTTGAAGCCATC	NM_001293757.1
	Antisense	GCTGCCTTTCATCGTCTTCT	
Arp1	Sense	ACTTGATTGGCGAGGAGAGT	NM_016860.1
	Antisense	TCACTCAGTAGCCTGTCTCCA	
Arp11	Sense	TGTGGTTATCGAGTCGGTGT	AF190797.1
	Antisense	CCAGGCTTTCCCTATATCCA	
CapZα	Sense	CAGTTCACACCCGTGAAGAT	NM_009797.2
	Antisense	CTCCCTCCAAGACTTCAAGC	
CapZβ	Sense	ACCCTCCTTTGGAAGATGG	NM_001037761.2
	Antisense	TGAGGATCACTCCAGCAAAG	
PAK1	Sense	TGCCGAGAGTGTCTACAAGC	NM_011035.2
	Antisense	CCATCCAATATGGAGTTCCC	
PAK2	Sense	AGAAGAAGAACCCTCAGGCA	NM_177326.3
	Antisense	GCAGCGTCTTCATCATCATC	
PAK3	Sense	ACATTGCGACTGGACAAGAG	NM_001195046.1
	Antisense	AAGAGCCACCAGCCAATAT	
PAK4	Sense	GAGAGAGTCCACCACCACCT	NM_027470.3
	Antisense	GACCATCCCTCGAAGATTTG	
PAK5	Sense	CAAGGAGTGATTCACAGGGA	NM_172858.2
	Antisense	GTCCCATAAGGTAGCCTGGA	
PAK6	Sense	CCTCTTCAAACCTGGTAGCC	NM_001033254.3
	Antisense	ATTGCTGGTGCTGATCTGAG	
NFATc1	Sense	CCAGTATACCAGCTCTGCCA	NM_016791.4
	Antisense	GTGGGAAGTCAGAAGTGGGT	
c-fos	Sense	ACTTCTTGTTTCCGGC	NM_010234
	Antisense	AGCTTCAGGGTAGGTG	
Ctsk	Sense	ATATGTGGGCCACCATGAAAGTT	NM_007802.4
	Antisense	TCGTTCCCCACAGGAATCTCT	
Cdc42	Sense	CAACAAACAAATTCCCATCGC	NM_009861.3
	Antisense	TGAGGATGGAGAGACCACTG	
Caspase-3	Sense	AAGGAGCAGCTTTGTGTGTG	NM_001284409.1
	Antisense	GTCTCAATGCCACAGTCCAG	
β-actin	Sense	TCTGGCACCACACCTTCTAC	NM_007393.5
	Antisense	TACGACCAGAGGCATACAGG	

III. Results

III.1. DCTN1 was increased at early stage upon RANKL stimulation

First, I examined the expression of dynactin subunits. BMMs were cultured for 2 days in the presence of M-CSF (30 ng/ml) and RANKL (200 ng/ml). Although CapZα and CapZβ were predominantly expressed among the whole components of dynactin complex (Fig. 5), the mRNA expression of DCTN1 was higher than other five DCTN family (Fig. 5). DCTN1 plays a most important role for dynactin functions (King and Schroer, 2000; Vaughan and Vallee, 1995). On the basis of these backgrounds, I focused on the role of DCTN1 in OC differentiation. I examined the expression of DCTN1 during OC differentiation. To investigate whether the expression of DCTN1 increased upon RANKL treatment, BMMs were cultured in the presence of M-CSF with or without RANKL for 48 hr. The protein level of DCTN1 was strongly increased at 9 hr after RANKL treatment and maintained at high levels for 48 hr during RANKL stimulation. (Fig. 6). To investigate whether DCTN1 expression was further increased during OC maturation, BMMs were cultured with M-CSF and RANKL to fully differentiate into OC. The protein level of DCTN1 was increased until BMMs commit to pre-fusion OC (pOC) and sustained during OC maturation (Fig. 7).

Since DCTN1 is a subunit of motor protein adaptor complex, its subcellular localization is diverse. Several reports have shown that dynactin was presented at many sites. Dynactin showed diverse localization at centrosome during cell division (Chen et al., 2015). The accumulation of dynactin was observed at microtubule plus ends that helps to endocytic trafficking (Valetti et al., 1999). Dynactin has also been observed on a variety of membrane organelles, including early/late endosomes, phagosomes, mitochondria, and also detected at membranes in the Golgi region in macrophages (Habermann et al., 2001). I investigated the subcellular localization of DCTN1 during osteoclastogenesis. Immunostaining with a DCTN1 specific antibody showed that DCTN1 expression was broadly detected at cytosol in BMMs and pOC. However, DCTN1 was restrictively localized within the cell periphery region and at the area surrounding outside of the nuclear membrane in mature OCs (Fig. 8).

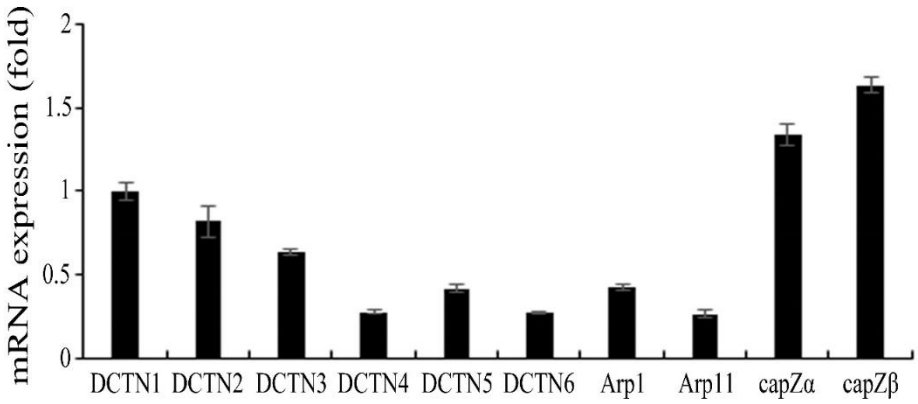

Figure 5. The mRNA expression of dynactin subunits in BMMs.

BMMs were cultured with M-CSF (30 ng/ml) and RANKL (200 ng/ml) for 2 days. The mRNA levels of DCTN1-6, Arp1/11 and CapZα/β were analyzed by real-time PCR.

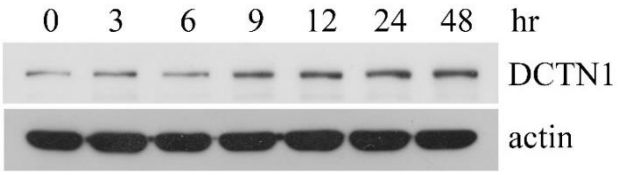

Figure 6. The induction of DCTN1 upon RANKL treatment.

BMMs were cultured with M-CSF (30 ng/ml) and RANKL (200 ng/ml) for the indicated time. The protein level of DCTN1 was detected by Western blotting.

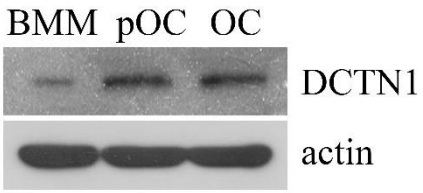

Figure 7. The protein level of DCTN1 during OC maturation.

BMMs were cultured with M-CSF (30 ng/ml) and RANKL (200 ng/ml) for 2 days (pOC) and 4 days (OC). The protein level of DCTN1 was determined by Western blotting. pOC, pre-fusion osteoclast; OC, osteoclast.

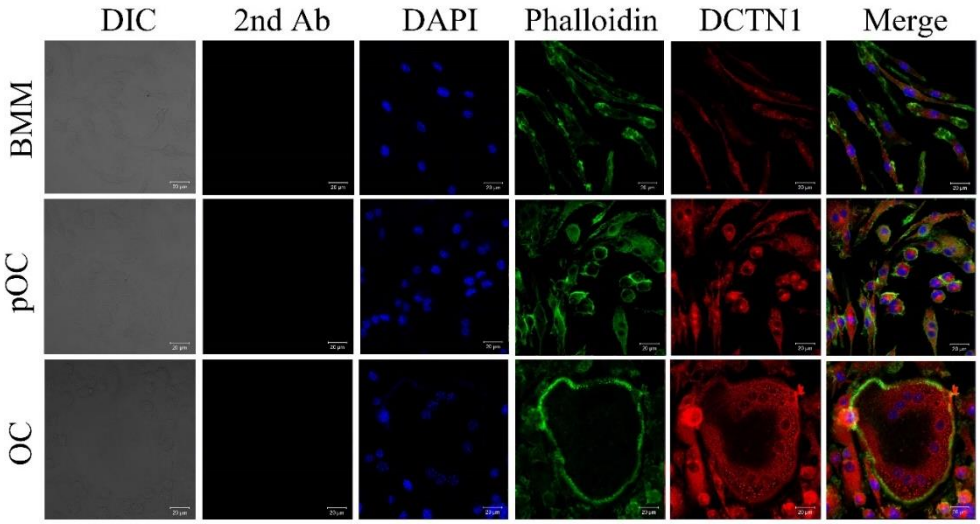

Figure 8. The subcellular localization of DCTN1 during osteoclastogenesis.

BMMs were cultured with M-CSF (30 ng/ml) and RANKL (200 ng/ml) for 2 (pOC, pre-fusion osteoclast) or 4 days (OC, osteoclast). Cells were immunostained using an antibody against DCTN1 followed by Cy3-conjugated secondary antibody. The membrane was stained with Alexa Fluor 633-conjugated phalloidin. DIC, differential interference contrast image; 2nd Ab, cells stained with secondary antibody only.

III.2. DCTN1 knockdown inhibited OC differentiation

To find the role of DCTN1 in OC differentiation, BMMs were transfected with specific siRNA against the DCTN1 or nonspecific siRNA as a control. Under the conditions where DCTN1 expression was efficiently suppressed, silencing of DCTN1 dramatically inhibited OC differentiation. The quantitative data also showed the decrease in the number of multinucleated cells (Fig. 9). NFATc1 and c-Fos are important transcriptional factors for osteoclast differentiation. In control cells, RANKL treatment increased NFATc1 and c-Fos at both mRNA and protein level. In contrast, DCTN1 knockdown reduced the RANKL effects on the induction of NFATc1 and c-Fos (Fig. 10A and B). NFATc1, in cooperation with MITF and PU.1, promotes the induction of genes for TRAP, MMPs, and Ctsk enzymes, which are important for OC functions. Next, I examined the mRNA expression of Ctsk which is an important enzyme for bone resorption, as a marker of OC differentiation. DCTN1 knockdown was decreased the gene expression of cathepsin K (Fig. 10B).

Since reduced OC differentiation would result in lower number of OC capable of resorbing bone, I performed resorption assay with dentin slices. BMMs transfected with control or DCTN1 siRNA were cultured on dentin slices for 9 days in the presence of M-CSF and RANKL. Consistent with the decrease in OC differentiation, DCTN1 knockdown significantly reduced resorbed area

(Fig. 11A). The depth of resorption pits was also reduced (Fig. 11A).

A reorganization of the actin cytoskeleton into a actin-ring structure is important for bone-resorbing function (Takahashi et al., 2007; Teitelbaum, 2000). I further investigated the effect of DCTN1 silencing on actin-ring formation, given the importance of this ring structure in the bone resorption process. I performed actin-ring staining with Alexa Fluor 633-conjugated phalloidin. In Fig. 11B, staining images showed the disruption of actin-ring formation in DCTN1-silenced OCs. The number of actin-ring-positive OCs was also reduced in DCTN1-silenced cells compared to control siRNA transfected cells. These results suggest that DCTN1 has a positive role for OC differentiation.

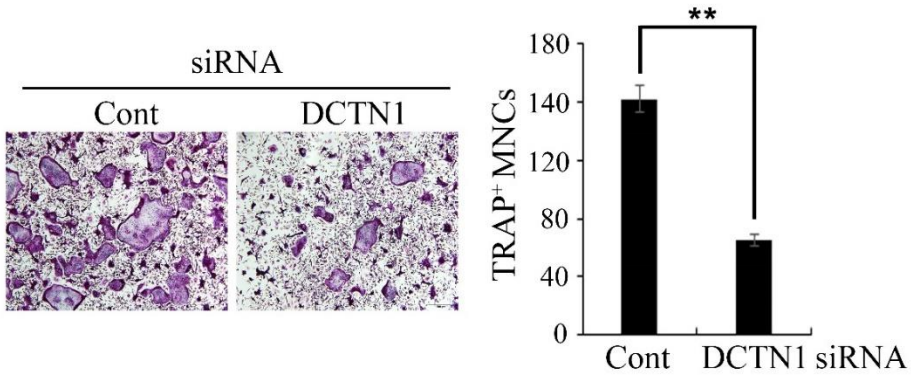

Figure 9. DCTN1 knockdown decreased OC differentiation.

BMMs transfected with control or DCTN1 siRNA were cultured with M-CSF (30 ng/ml) and RANKL (200 ng/ml) for 4 days and stained for TRAP. TRAP-positive multinucleated cells were counted. **, $p < 0.005$ as compared to controls. Cont, control siRNA; DCTN1, DCTN1 siRNA.

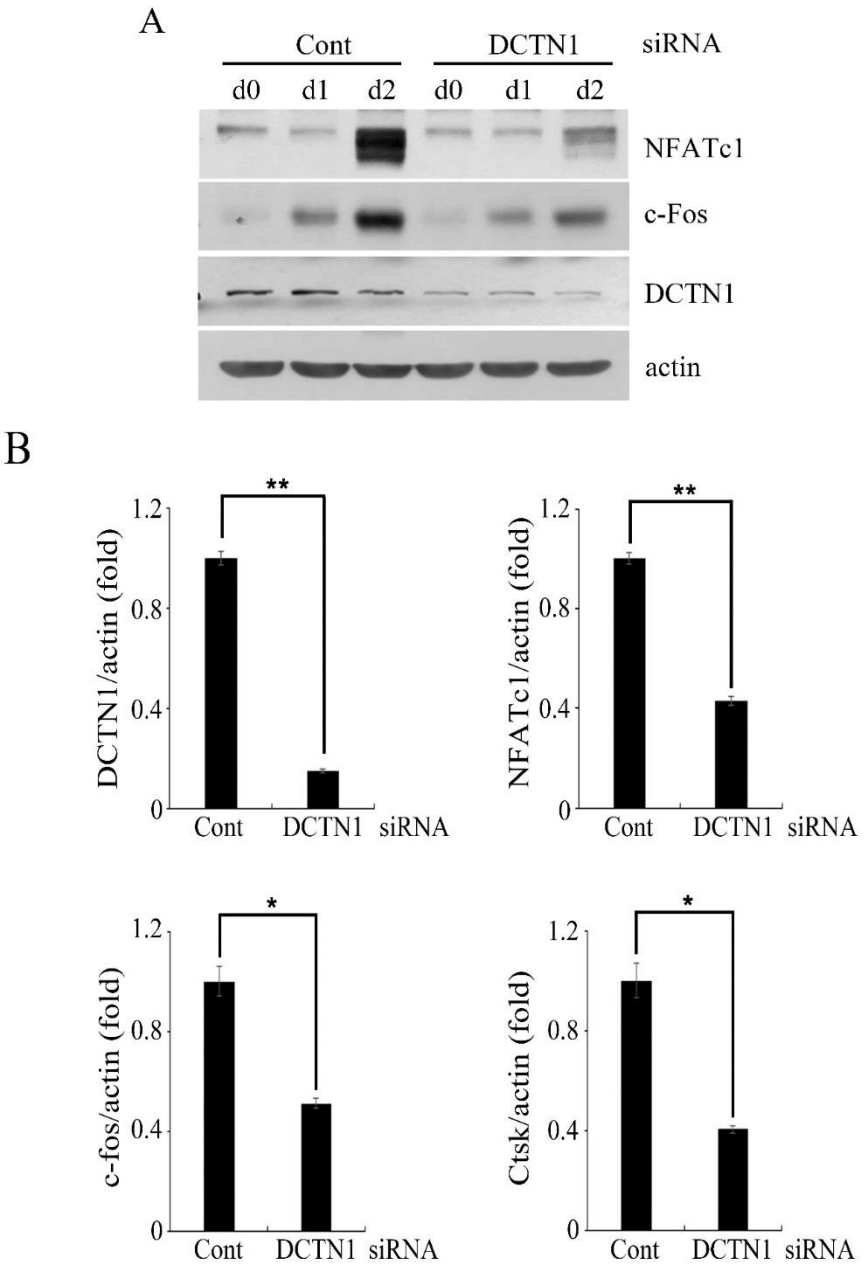

Figure 10. Induction of NFATc1 and c-Fos was inhibited by DCTN1 knockdown.

(A) BMMs transfected with control or DCTN1 siRNA were cultured with M-CSF (30 ng/ml) and RANKL (200 ng/ml) for the indicated days. Whole cell lysates were subjected to Western blotting with anti-NFATc1, anti-c-Fos and anti-DCTN1. (B) BMMs transfected with control or DCTN1 siRNA were cultured with M-CSF (30 ng/ml) and RANKL (200 ng/ml) for 48 hr, the mRNA levels of NFATc1, c-Fos, Ctsk and DCTN1 were analyzed by real-time PCR. *, $p < 0.005$; **, $p < 0.0005$ as compared to controls. Cont, control siRNA; DCTN1, DCTN1 siRNA.

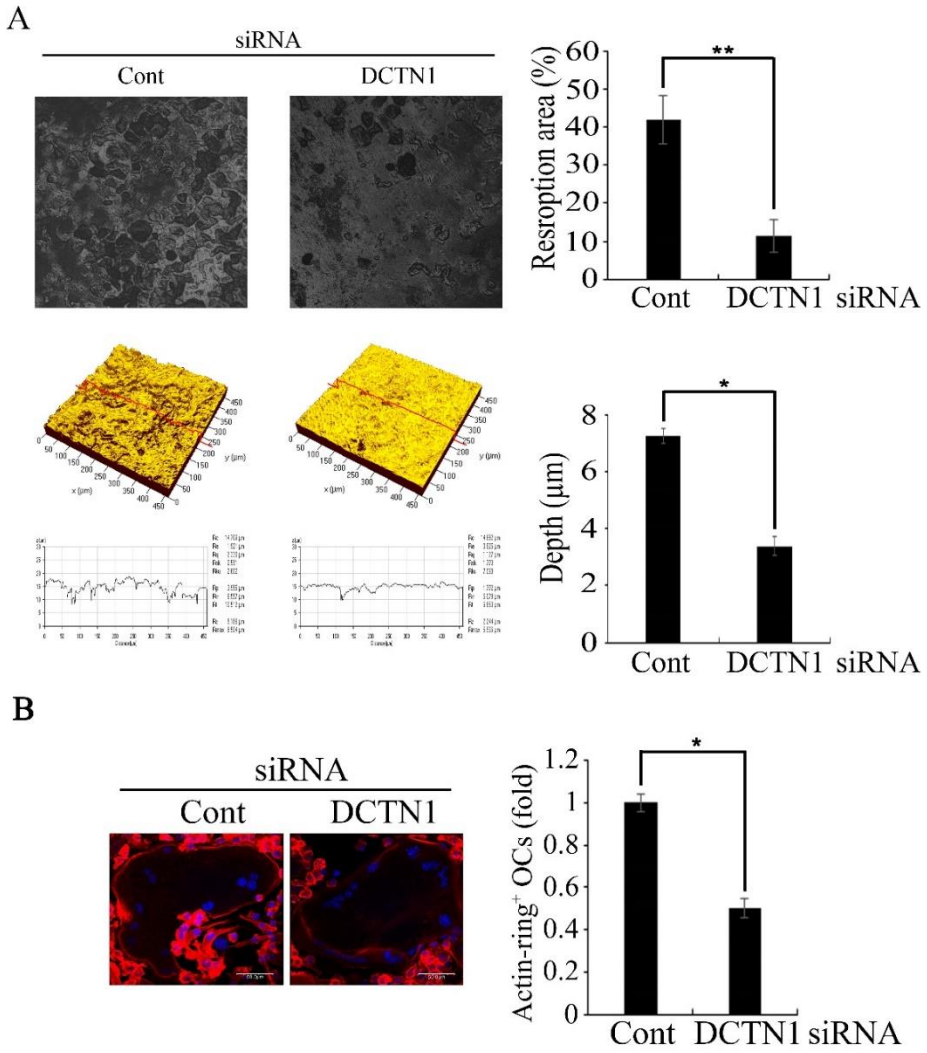

Figure 11. DCTN1 knockdown reduced bone resorption and actin-ring formation.

(A) BMMs transfected with control or DCTN1 siRNA were cultured on dentin

slices in the presence of M-CSF (30 ng/ml) and RANKL (200 ng/ml) for 9 days. Black areas indicate resorbed surface on dentin slices. The quantitative data of the resorption area and depth were measured from randomly selected four images. (B) BMMs transfected with control or DCTN1 siRNA were cultured on dentine slices in the presence of M-CSF (30 ng/ml) and (200 ng/ml) for 4 days. Cells were stained with Alexa Fluor 633-conjugated phalloidin. The quantitative data of relative comparison of actin-ring positive OCs between control and DCTN1 knockdown cells were measured by counting OCs with intact actin-ring per total OCs from randomly selected four images. *, $p < 0.05$; **, $p < 0.005$ as compared to controls. Cont, control siRNA; DCTN1, DCTN1 siRNA.

III.3. DCTN1-silenced BMMs showed abnormal RANKL signaling

RANKL stimulates the activation of MAPKs involving ERK1/2, p38, and JNK, which is essential for increasing NFATc1 induction. The Akt pathways also have an important role for survival and differentiation of OC precursor cells and are required for the induction of NFATc1 (Asagiri and Takayanagi, 2007; Takayanagi, 2007). MAPKs have an important role in OC differentiation. The MAPKs have been reported to be activated by RANKL stimulation, which promote the activation of activating protein 1 (AP-1) complex. AP-1 complex containing c-Fos and c-Jun is required for the induction of NFATc1, a key transcription factor for OC differentiation. MAPKs have been involved in the induction of c-Fos (Huang et al., 2006; Lee et al., 2010). JNK has been implicated in the induction of c-Jun phosphorylation (Ikeda et al., 2004)

To determine the effect of DCTN1 on the intracellular signaling, I investigated the activation of MAPK and Akt signaling pathways upon RANKL stimulation. The activation of ERK, p38, and JNK was determined by Western blot analysis using antibodies specifically directed against the phosphorylated forms. The phosphorylation of all three MAPKs and Akt induced by RANKL at 5 and 15 min (Fig. 12). However, DCTN1 knockdown reduced the phosphorylation of ERK1/2, p38, and Akt upon RANKL treatment. On the contrary, the phosphorylation of JNK was increased by DCTN1 knockdown (Fig.

12). Therefore, it is likely that the disruption of the MAPK and Akt pathways decreased NFATc1 and c-Fos induction, resulting in the suppression of osteoclastogenesis by DCTN1 knockdown.

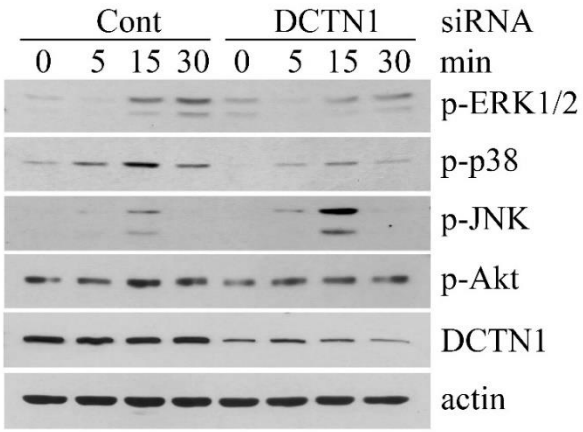

Figure 12. The disruption of RANKL-induced signal transduction by DCTN1 knockdown.

BMMs were transfected with control or DCTN1 siRNA. Cells were treated with RANKL (400 ng/ml) after serum starvation for 6 hr. The phosphorylation of ERK1/2, p38, JNK, and Akt was determined by Western blotting. Cont, control siRNA; DCTN1, DCTN1 siRNA.

III.4. DCTN1 regulates the activation of Cdc42 during OC differentiation

To find the mechanism of DCTN1-mediated regulation of OC differentiation, I focused on small GTPases which are important regulators of the actin cytoskeleton. They play multiple roles in cell regulation (Jaffe and Hall, 2005). Cdc42 has been implicated in cell differentiation. For an example, differentiation of hair follicle cells from skin stem cells requires Cdc42 regulation of β-catenin turnover (Wu et al., 2006). In a previous report, Cdc42 was shown to be involved in osteoclastogenesis, positively regulating MAPK pathways (Ito et al., 2010). Based on the these reports, I investigated whether DCTN1 knockdown affected Cdc42 activity. BMMs transfected with control or DCTN1 siRNA were stimulated with RANKL after serum starvation 4 hr and pull-down assay was performed with beads conjugated with p21-binding domain (PBD) fused GST. As shown in Fig. 13A, knockdown of DCTN1 significantly reduced the level of GTP-bound Cdc42. However, the activation of Rac1, another GTPase protein, which was reported to regulate OC differentiation (Lee et al., 2006; Wang et al., 2008), was not affected by DCTN1 knockdown (Fig. 13B).

I next investigated whether Cdc42 activation was an essential factor for the regulation of DCTN1-dependent OC differentiation. To verify this hypothesis, constitutively active Cdc42 (Q61L) was overexpressed in DCTN1-silenced BMM. BMMs were infected with control or Q61L-containing retrovirus. The

efficiency of retrovirus infection was verified by Western blotting (Fig. 14A). OC differentiation impaired by DCTN1 silencing was restored by the overexpression of Cdc42 Q61L (Fig. 14B). The inhibition of NFATc1 and c-Fos expression, when DCTN1 was silenced, were also recovered at both mRNA and protein level (Fig. 15A and B). Next, I investigated the effect of Cdc42 Q61L overexpression on RANKL-induced signaling pathways. The reduction in the phosphorylation of ERK1/2, p38, and Akt was rescued by Cdc42 Q61L overexpression (Fig. 16). JNK phosphorylation was also reversed when Cdc42 Q61L was overexpressed (Fig. 16). These results indicated that DCTN1 mainly regulates the RANKL-mediated signaling pathways and OC differentiation through the activation of Cdc42.

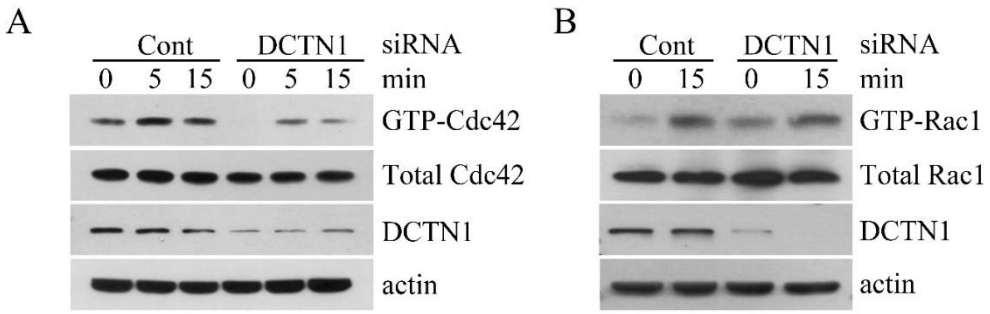

Figure 13. DCTN1 knockdown significantly inhibited Cdc42 activation.

(A, B) BMMs were transfected with control or DCTN1 siRNA. After serum starvation for 4 hr, cells were treated with RANKL (400 ng/ml) for the indicated times. The activated Cdc42 or Rac1 was precipitated using PBD-GST beads. The levels of GTP-Cdc42 or GTP-Rac1 were determined by Western blotting. The levels of total Cdc42 or Rac1 were detected by Western blotting using whole cell lysates. Cont, control siRNA; DCTN1, DCTN1 siRNA.

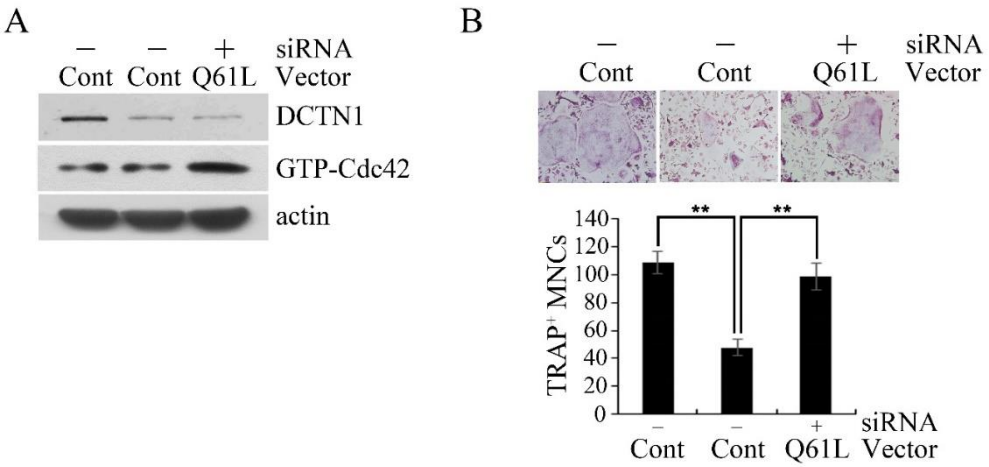

Figure 14. The overexpression of constitutively activate Cdc42 (Q61L) in DCTN1-silenced BMMs rescued OC differentiation.

(A) BMMs transfected with DCTN1 siRNA were infected with supernatant-containing Cdc42 Q61L-harboring retrovirus. The protein level of DCTN1 was detected by Western blotting. GTP-Cdc42 precipitated with PBD-beads were detected by Western blotting. (B) BMMs transfected with DCTN1 siRNA were infected with supernatant-containing Cdc42 Q61L-harboring retrovirus. Cells were then cultured with M-CSF (30 ng/ml) and RANKL (200 ng/ml) for 4 days and stained for TRAP. TRAP-positive multinucleated cells were counted. **, $p < 0.005$ as compared to controls. Cont, control pMX vector; Q61L, pMX vector containing constitutively active Cdc42.

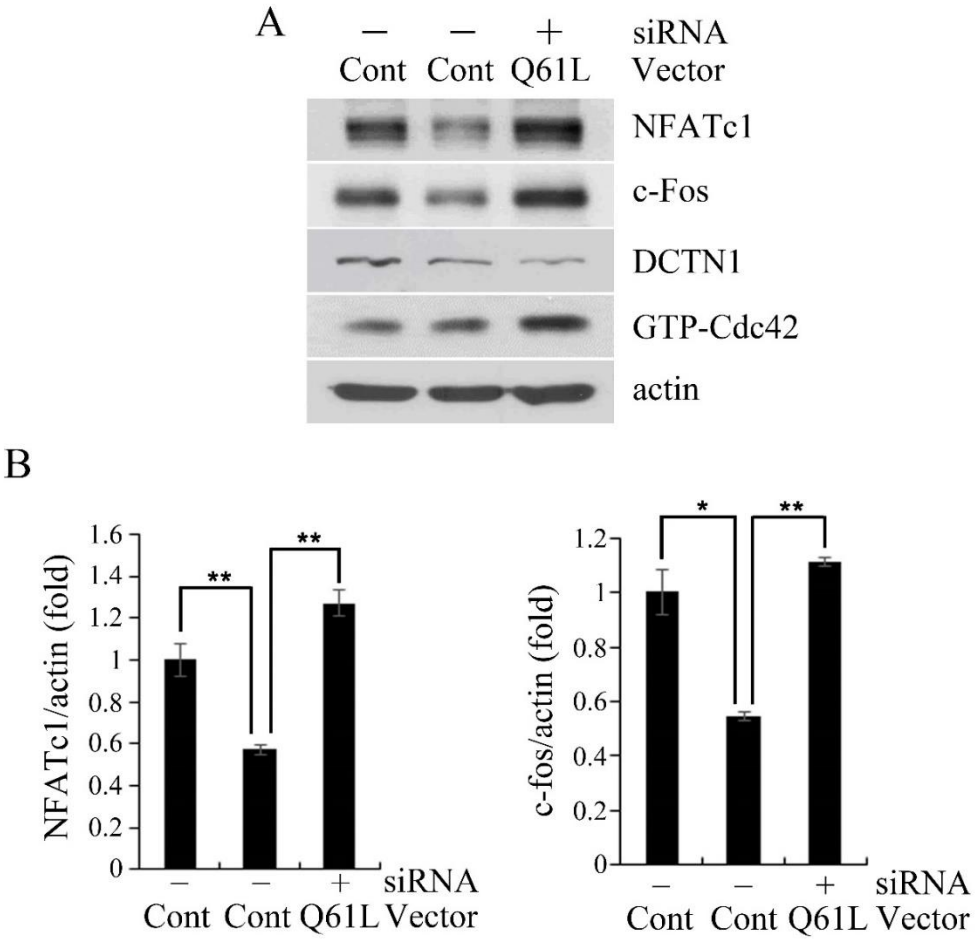

Figure 15. Forced expression of Cdc42 Q61L in DCTN1-silenced BMMs increased NFATc1 and c-Fos.

BMMs transfected with DCTN1 siRNA were infected with supernatant-containing Cdc42 Q61L-harboring retrovirus. Cells were further cultured with M-CSF (30 ng/ml) and RANKL (200 ng/ml) for 48 hr. (A) The protein levels of

NFATc1 and c-Fos were determined by Western blotting. (B) The mRNA expression of NFATc1 and c-Fos was analyzed by real-time PCR (right panel). *, $p < 0.05$; **, $p < 0.005$ as compared to controls. Cont, control pMX vector; Q61L, pMX vector containing constitutively active Cdc42.

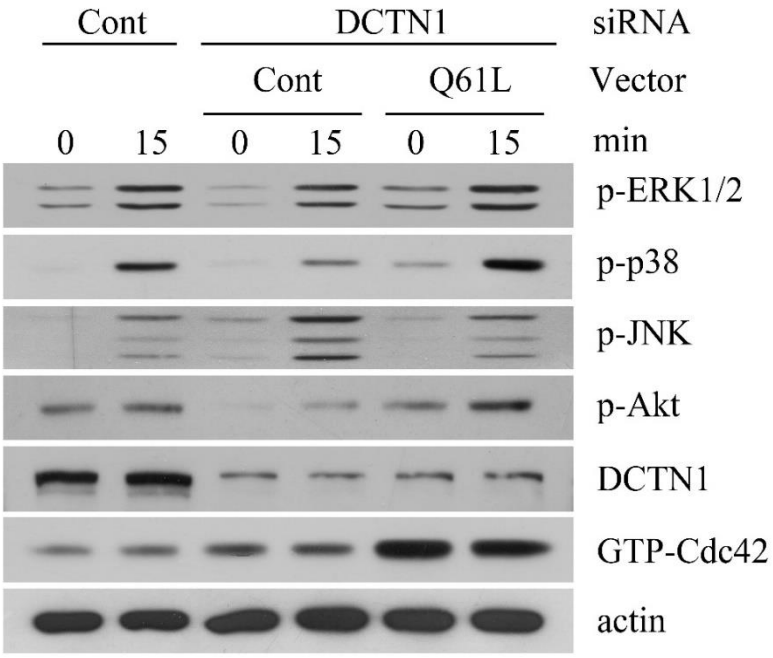

Figure 16. The effect on RANKL-induced signaling pathways of Cdc42 Q61L overexpression in DCTN1-silenced BMMs.

BMMs transfected with DCTN1 siRNA were infected with supernatant-containing Cdc42 Q61L-harboring retrovirus. Cells were treated with RANKL (400 ng/ml) after serum starvation for 6 hr. The phosphorylation of ERK1/2, p38, JNK, and Akt was determined by Western blotting. Cont, control pMX vector; Q61L, pMX vector containing constitutively active Cdc42.

III.5. The activation of Cdc42 was Src-independently regulated by DCTN1

Src kinases have been involved intracellular signaling through association with diverse receptors and intracellular membrane proteins (Thomas and Brugge, 1997). The Cdc42 has also been implicated in Src kinase-related cellular events. For an example, endothelin, a GPCR ligand, inhibited cell motility through activation of JNK pathway. This effect was mediated by Src kinase and small GTPase Cdc42 (Yamauchi et al., 2002). Src kinase has been shown to be involved in Cdc42 activation in epithelial cells through nectin, a Ca^{2+}-independent Ig-like cell-cell adhesion molecule. Src was recruited and activated by nectin mediated cell–cell adhesion. Then, FRG was subsequently recruited and phosphorylated by Src. The activation of FRG increased GTP-bound Cdc42 (Fukuhara et al., 2004). Cdc42 and Src kinase also have an important role for OC differentiation and function, respectively (Ito et al., 2010; Miyazaki et al., 2004).

I examined whether the inhibition of Cdc42 activation arises from the alteration of Src activity by DCTN1 knockdown. I determined Src activation with specific antibody which recognizes phosphorylated Tyr416. Phosphorylation on this residue is known to activate Src (Hunter, 1987). DCTN1 knockdown did not inhibited, rather slightly increased the Src phosphorylation upon RANKL treatment (Fig. 17A). Next, I investigated whether silencing of Src inhibits the activation of Cdc42. BMMs transfected with Src siRNA were stimulated by

RANKL after serum starvation for 4 hr. As expected, the level of GTP-bound Cdc42 was significantly decreased in Src siRNA transfected BMMs compared with control siRNA transfected BMMs (Fig. 17B). Although, Src ascted as an upstream of Cdc42 pathway, it is likely that the decrease of GTP-bound Cdc42 Src-independently regulated by DCTN1.

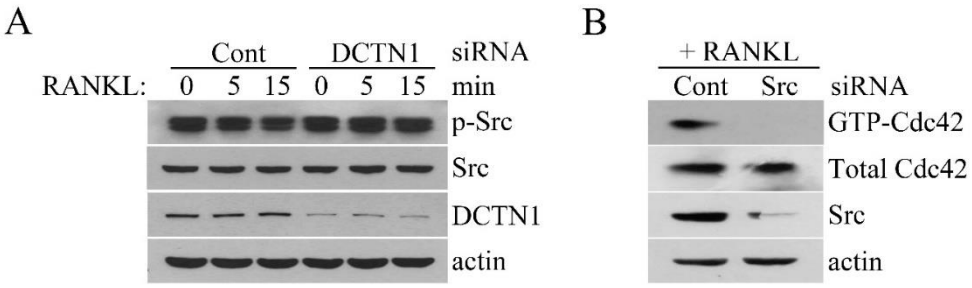

Figure 17. Src kinase was not involved in DCTN1-mediated Cdc42 activation.

(A) BMMs were transfected with control or DCTN1 siRNA. Cells were treated with RANKL (400 ng/ml) after serum starvation for 4 hr. The phosphorylation of Src was determined by Western blotting. (B) BMMs were transfected with control or Src siRNA. Cells were treated with RANKL (400 ng/ml) for the indicated time after serum starvation for 4 hr. The active Cdc42 was precipitated using PBD-fusion GST bead. The levels of GTP-Cdc42 and Src were determined by Western blotting. Cont, control siRNA; DCTN1, DCTN1 siRNA; Src, Src siRNA.

III.6. Cdc42/PAK2 axis positively regulated osteoclastogenesis

Members of p21-activated kinase (PAK) family, serine/threonine kinases, are involved in diverse cellular processes and are regulated by the small GTPase protein family (Rane and Minden, 2014). The six members of PAK family are classified into two groups - group I (PAK1, PAK2 and PAK3), and group II (PAK4, PAK5, and PAK6) according to the structural and functional similarities (Li et al., 2010). G protein-coupled receptor and receptor tyrosine kinase lead to activation of PAKs (Knaus et al., 1995; Tsakiridis et al., 1996). These pathways generally activate PAKs through sequential activation of PI3 kinase (PI3K). Activated PAKs mediated Rac and Cdc42 signaling, small GTPases (Dummler et al., 2009)).

Since DCTN1 affected the activation of Cdc42, I hypothesized that DCTN1 silencing affects PAKs activation. First, I examined the mRNA expression of the six PAK family members during osteoclastogenesis. Among the 6 isoforms, PAK1, 2, and 4 were mainly expressed during OC differentiation by RANKL. PAK2 was expressed at the highest level (Fig. 18). To find which isoform acts as a common downstream effector of both DCTN1 and Cdc42 signaling, I next investigated whether depletion of DCTN1 or Cdc42 affects the phosphorylation of PAK isoforms. BMMs were transfected with DCTN1 or Cdc42 siRNA. Then, cells were stimulated with RANKL after serum starvation for 6 hr. RANKL-

induced PAK2 phosphorylation was increased in control siRNA transfected BMMs. In contrast, the phosphorylation of PAK2 was dramatically inhibited by DCTN1 siRNA (Fig. 19). However, the phosphorylation of PAK 1 and 4 in response to RANKL was comparable between control and DCTN1 knockdown cells. Silencing of Cdc42 also affected PAK2 phosphorylation (Fig. 19). Since PAK2 activation was inhibited by both DCTN1 and Cdc42 siRNA, we next examined the role of PAK2 in OC differentiation. PAK2 siRNA transfected BMMs were cultured with RANKL for 4 days. PAK2 silencing reduced OC differentiation (Fig. 20A). The mRNA expression of NFATc1 was also reduced (Fig. 20B). The RANKL signaling pathways were also disrupted by PAK2 knockdown (Fig. 21). The phosphorylation of ERK1/2, p38, and JNK was decreased by PAK2 knockdown. However, Akt phosphorylation was slightly increased by PAK2 knockdown (Fig. 21).

PAKs, cooperating with Rac1 or Cdc42, also participate in the regulation of cytoskeleton organization (Sells et al., 1997). Since the regulation of cytoskeleton organization is important for osteoclast function, I next investigated the involvement of PAK2 in bone resorption and actin-ring formation. PAK2 siRNA transfected BMMs was differentiated into OCs on dentin slices for 9 days in the presence of M-CSF and RANKL. Fig. 22A shown that the reduction of osteoclastic resorption on dentin slices. Resorbed area and depth of resorption

pits were also reduced by PAK2 silencing (Fig. 22A). The number of mature OC with intact actin-ring structure were also decreased by PAK2 knockdown (Fig. 22B). These results indicate that PAK2, which acts as a downstream effector of Cdc42, has a positive role in osteoclastogenesis.

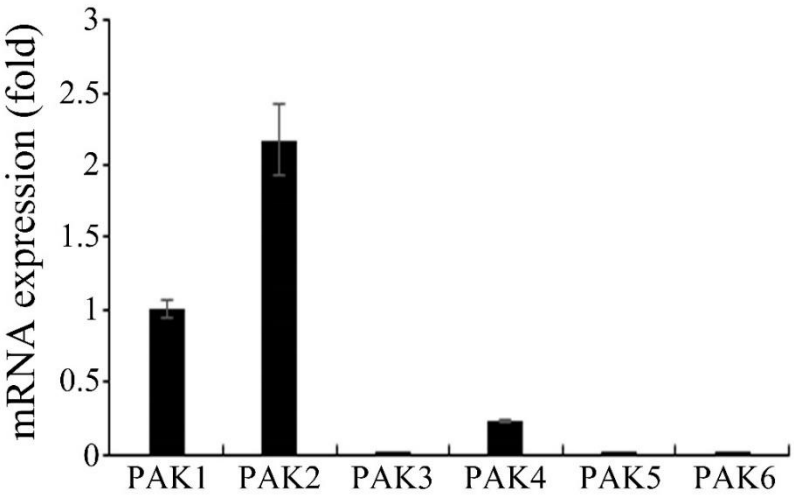

Figure 18. The gene expression of p21-activated kinase family members by RANKL.

BMMs were treated with M-CSF (30 ng/ml) and RANKL (200 ng/ml) for 48 hr. The mRNA expression of PAK1-6 was analyzed by real-time PCR.

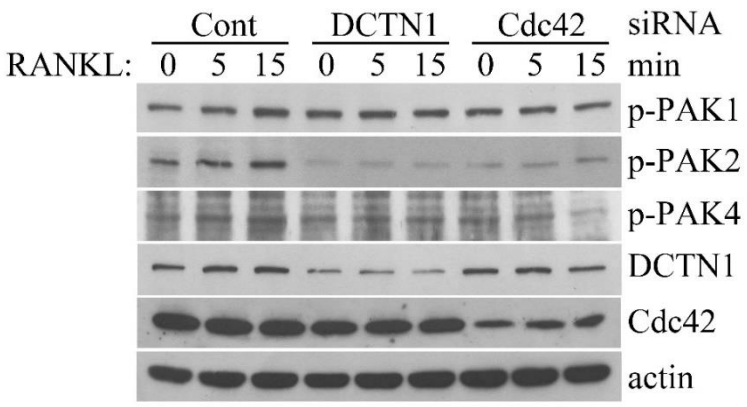

Figure 19. DCTN1 or Cdc42 knockdown inhibited PAK2 phosphorylation by RANKL.

BMMs were transfected with control or DCTN1 or Cdc42 siRNA for 24 hr. Cells were treated with RANKL (400 ng/ml) for the indicated time after serum starvation for 6 hr. The phosphorylation of PAK1, PAK2, and PAK4 was determined with anti-phospho-PAK1, anti-phospho-PAK2, and anti-phospho-PAK4 by Western blotting. Cont, control siRNA; DCTN1, DCTN1 siRNA; Cdc42, Cdc42 siRNA.

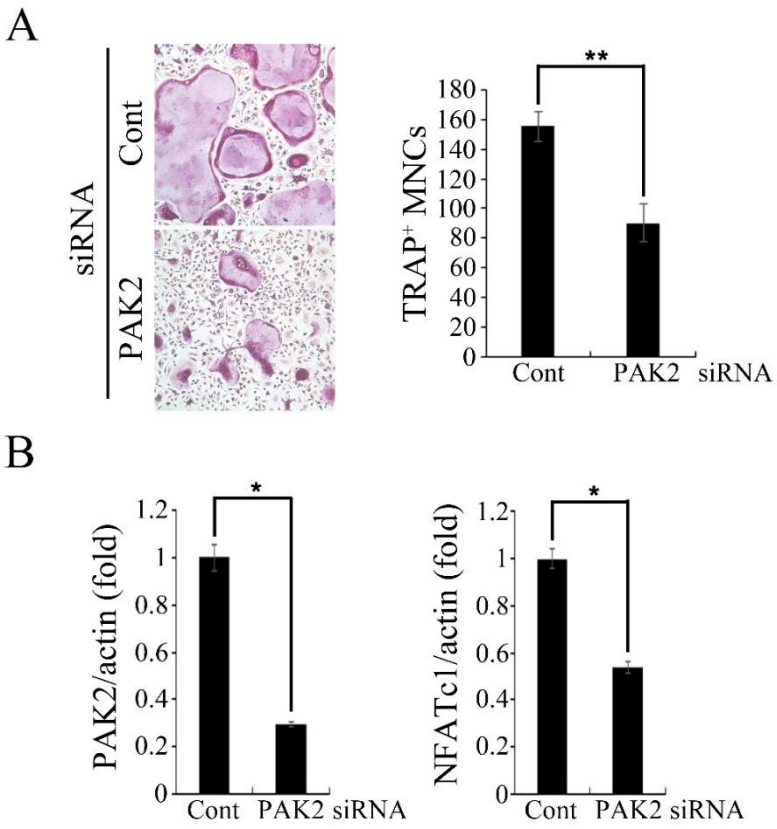

Figure 20. PAK2 knockdown reduced OC differentiation.

(A) BMMs were transfected with control or PAK2 siRNA for 24 hr. Cells were cultured in the presence of M-CSF (30 ng/ml) and RANKL (200 ng/ml) for 4 days and stained for TRAP. TRAP-positive multinucleated cells were counted. (B) BMMs were transfected with control or PAK2 siRNA for 24 hr. Cells were cultured in the presence of M-CSF (30 ng/ml) and RANKL (200 ng/ml) for 48

hr. The mRNA expression of PAK2 and NFATc1 was analyzed by real-time PCR. *, $p < 0.005$; **, $p < 0.0005$ as compared to controls. Cont, control siRNA; PAK2, PAK2 siRNA.

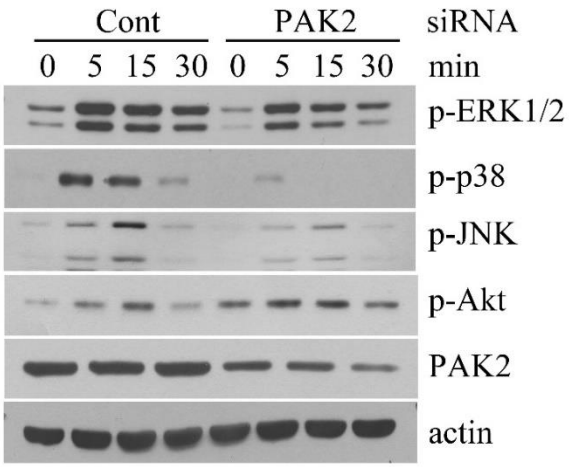

Figure 21. PAK2 knockdown disrupted MAPK and Akt signaling.

BMMs were transfected with control or PAK2 siRNA for 24 hr. Cells were treated with RANKL (400 ng/ml) after serum starvation for 6 hr. The phosphorylation of ERK1/2, p38, JNK, and Akt was determined by Western blotting.

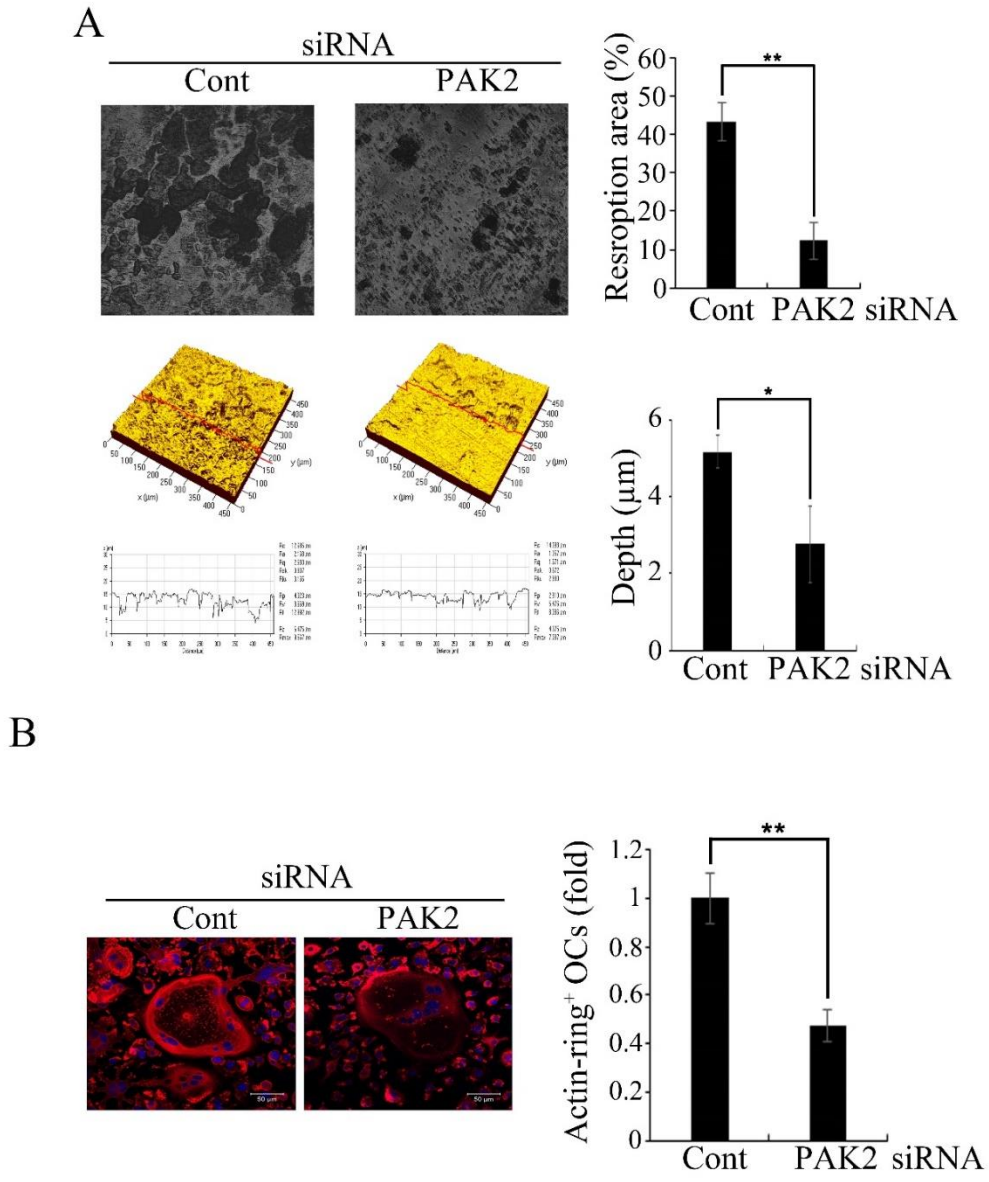

Figure 22. PAK2 knockdown reduced bone resorption and actin-ring formation.

(A) BMMs transfected with control or PAK2 siRNA for 24 hr. Cells were cultured on dentin slices in the presence of M-CSF (30 ng/ml) and RANKL (200 ng/ml) for 9 days. Black areas indicate resorbed surface on dentin slices. The quantitative data of the resorption area and depth were measured from randomly selected four images. (B) BMMs were transfected with control or PAK2 siRNA for 24 hr. Cells were cultured on dentin slices in the presence of M-CSF (30 ng/ml) and RANKL (200 ng/ml) for 4 days. Cells were stained with Alexa Fluor 633-conjugated phalloidin. The quantitative data of relative comparison of actin-ring positive OCs between control and DCTN1 knockdown cells were measured by counting OCs with intact actin-ring per total OCs from randomly selected four images. *, $p < 0.05$; **, $p < 0.005$ as compared to controls. Cont, control siRNA; PAK2, PAK2 siRNA.

III.7. DCTN1-silenced OC precursor cells were susceptible to apoptosis

It has been reported that DCTN1 is involved in cell division (Karki and Holzbaur, 1999). It is well known that the reduced proliferation of OC precursor cells affects OC formation. Therefore, I investigated whether DCTN1 knockdown affects the viability of OC precursor cells. The proliferation of DCTN1-silenced BMMs began to decline at 2 days after RANKL treatment and this deviation was more increased at 3 days (Fig. 23). Next, I examined whether DCTN1 knockdown affects the indicators of cell proliferation and apoptosis. The expression of cyclin D1, a proliferation marker, was not altered (Fig. 24A). However, DCTN1 silencing in BMMs promoted cleavage of caspase-3, an executor of apoptosis, upon RANKL treatment (Fig. 24A). These results suggest that DCTN1-silencing increased apoptosis of OC precursor cells upon RANKL treatment. Additionally, I found that the number of TUNEL-positive apoptotic OC precursor cells was increased by DCTN1 knockdown (Fig. 24B). Since DCTN1 knockdown inhibited Cdc42 activation (Fig. 13A), I examined the effect of Cdc42 silencing on the cell death. Apoptotic OC precursors were also increased in Cdc42-silenced cells (Fig 24B). Although the activated caspase-3 was increased by DCTN1 silencing, pro-caspase-3 was simultaneously increased by DCTN1 knockdown. To investigate the elevation of cleaved caspase-3 arises from its transcriptional modulation, I examined the alteration of caspase-3 mRNA

expression. The mRNA level of caspase-3 was upregulated by silencing of both DCTN1 and Cdc42 (Fig. 25). These results suggest that caspase-3 was regulated at the transcriptional level by DCTN1 knockdown.

Hematopoietic lineage-specific signal transducer and activator of transcription 3 (STAT3) knockout mice showed an osteoporotic phenotype with increased OCs which was induced by hyperproliferation of the Mac1+ and c-kit+ myeloid lineage cells (Zhang et al., 2005). Moreover, a recent study showed that phospho-STAT3 binds to the caspase-3 promoter region and promotes its transcription in muscle cells (Silva et al., 2015). I examined whether DCTN1 knockdown affects STAT3 activation. RANKL-stimulation of DCTN1-silenced BMMs increased STAT3 phosphorylation (Fig. 26).

To verify whether the enhancement of OC precursor cell death leads to failure of the OC generation, BMMs transfected with DCTN1 siRNA were cultured in the presence or absence of Z-DEVD-FMK, a caspase-3 inhibitor, during OC differentiation. The treatment inhibited the cleavage of caspase-3 (Fig 27.C). However, Z-DEVD-FMK treatment could not fully recover OC generation (Fig. 27A and B). It suggests that the enhanced apoptosis of OC precursor cells only partially contributed to the inhibition OC differentiation by DCTN1 knockdown. In Fig. 12, the level of phosphorylated JNK was increased by DCTN1 silencing, unlike that of ERK1/2 or p38. A previous report showed that RANKL-mediated

JNK activation induced apoptosis in NF-κB $p65^{-/-}$ mice (Vaira et al., 2008). To examine whether the impairment of OC differentiation arises from the elevation of JNK activation by DCTN1 silencing, DCTN1 silenced BMMs were cultured with or without SP600125, a JNK inhibitor, in the presence of M-CSF and RANKL. The OC differentiation was not rescued by JNK inhibition (Fig. 28A and B). The cleavage of caspase-3 was not also inhibited (Fig. 28C). These results indicate that JNK was not involved in RANKL-induced apoptosis in DCTN1 knockdown BMMs.

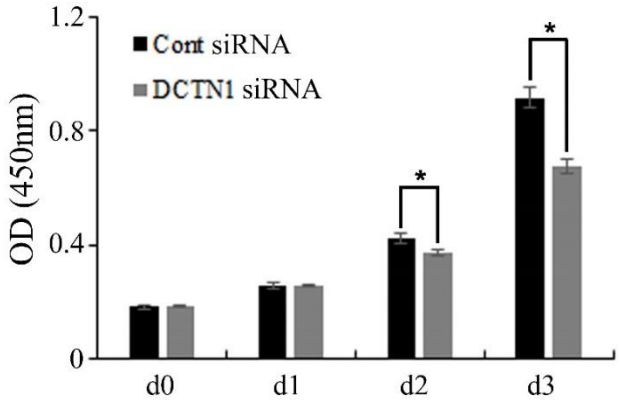

Figure 23. DCTN1 knockdown inhibited cell viability of OC precursor cells.

BMMs were transfected with control or DCTN1 siRNA for 24 hr and further cultured in the presence of M-CSF (30 ng/ml) and RANKL (200 ng/ml) for the indicated days. Cells were incubated with culture medium containing 10% CCK reagent for 1 hr at 37℃. Cell viability was measured with an ELISA reader at 450 nm. *, $p < 0.05$ as compared to controls.

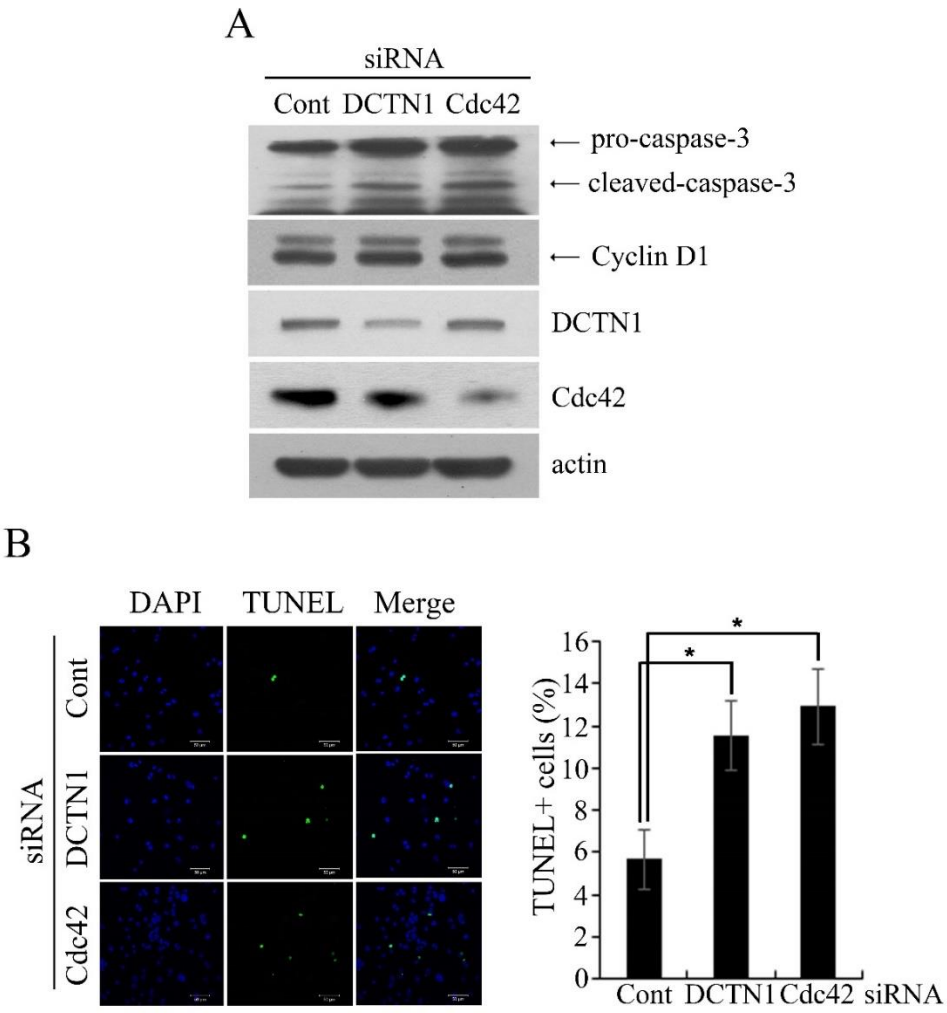

Figure 24. DCTN1 or Cdc42 depletion increased apoptosis during OC differentiation.

(A) BMMs were transfected with control, DCTN1, or Cdc42 siRNA for 24 hr. Cells were treated with M-CSF (30 ng/ml) and RANKL (200 ng/ml) for 48 hr.

The protein levels of Caspase-3, DCTN1, and Cdc42 were detected by Western blotting. (B) TUNEL assay was performed with DCTN1 or Cdc42 siRNA-transfected BMMs after treatment with M-CSF (30 ng/ml) and RANKL (200 ng/ml) for 2 days. TUNEL-positive cells were counted . *, $p < 0.05$ as compared to controls. Cont, control siRNA; DCTN1, DCTN1 siRNA; Cdc42, Cdc42 siRNA.

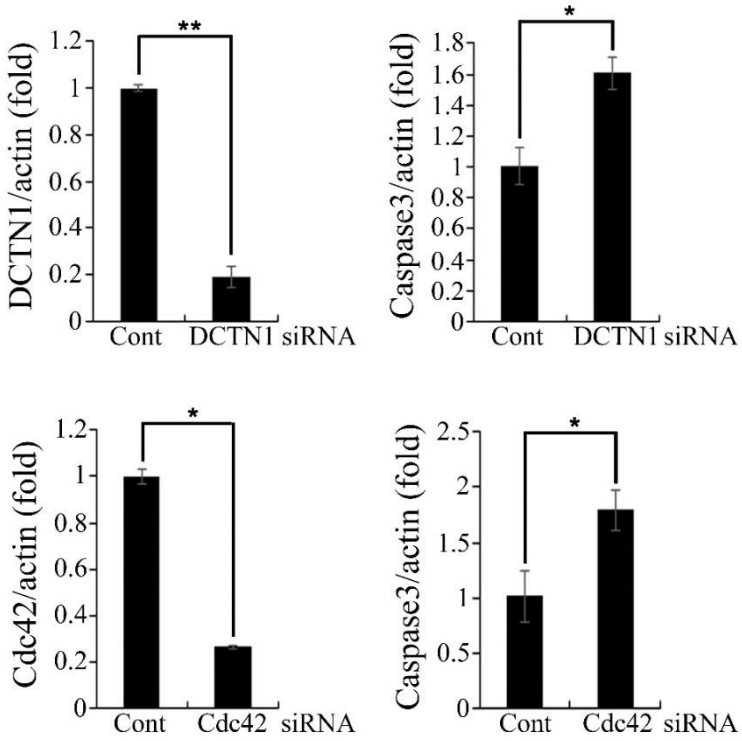

Figure 25. DCTN1 or Cdc42 knockdown inhibited the mRNA expression of caspase-3 by RANKL.

BMMs were transfected with control, DCTN1, or Cdc42 siRNA for 42 hr. Cells were cultured with M-CSF (30 ng/ml) and RANKL (200 ng/ml) for 48 hr. The level of caspase-3 mRNA was analyzed by real-time PCR. *, $p < 0.05$; **, $p < 0.005$ as compared to controls. Cont, control siRNA; DCTN1, DCTN1 siRNA; Cdc42, Cdc42 siRNA.

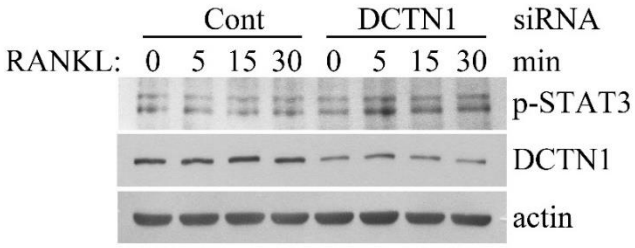

Figure 26. DCTN1 knockdown upregulates the phosphorylation of STAT3.

BMMs were transfected with control or DCTN1 siRNA for 24 hr. Cells were treated with RANKL (400 ng/ml) after serum starvation for 6 hr. The phosphorylation of STAT3 was determined by Western blotting. Cont, control siRNA; DCTN1, DCTN1 siRNA.

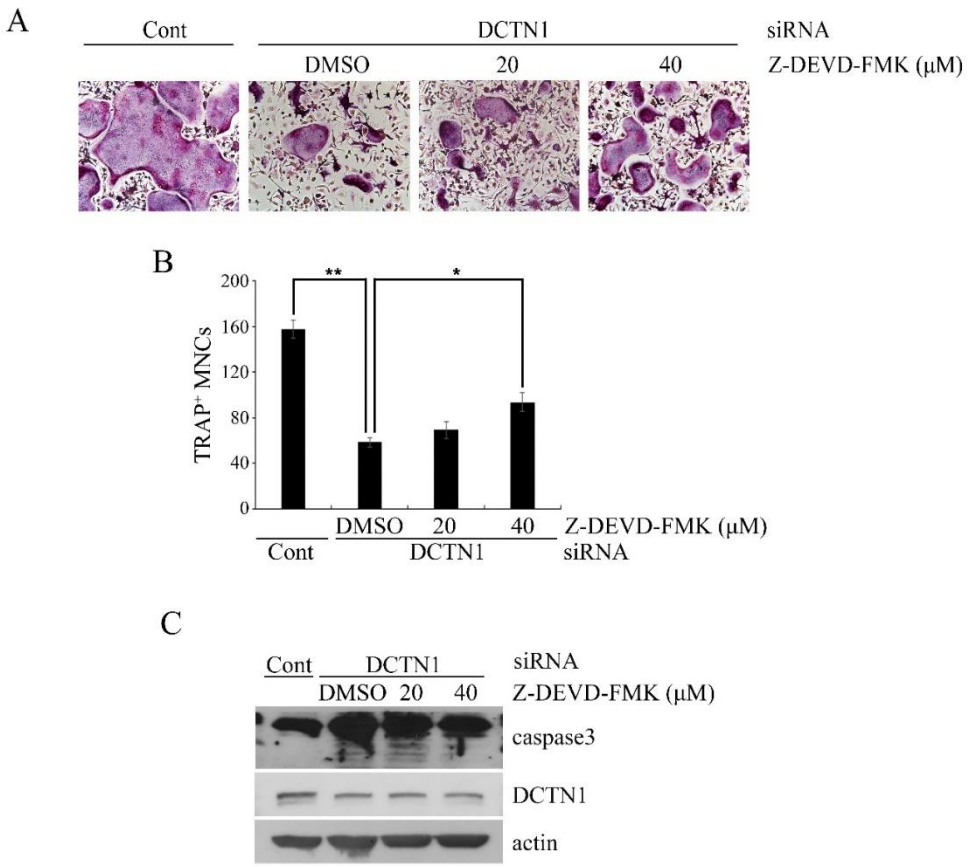

Figure 27. RANKL-induced cell death in DCTN1-silence BMMs was partially recovered by caspase-3 inhibition.

(A) BMMs were transfected with control or DCTN1 siRNA for 24 hr. Cells were cultured in the presence of M-CSF (30 ng/ml) and RANKL (200 ng/ml) for 4 days with or without Z-DEVD-FMD during the first 48 hr for the indicated dose.

(B) TRAP-positive multinucleated cells were counted. (C) BMMs were transfected with control or DCTN1 siRNA for 24 hr. Cells were cultured in the presence of M-CSF (30 ng/ml) and RANKL (200 ng/ml) for 48 hr with or without Z-DEVD-FMD for the indicated dose. Caspase-3 and DCTN1 were detected by Western blotting. *, $p < 0.005$ as compared to DMSO, **, $p < 0.0005$ as compared to controls. Cont, control siRNA; DCTN1, DCTN1 siRNA.

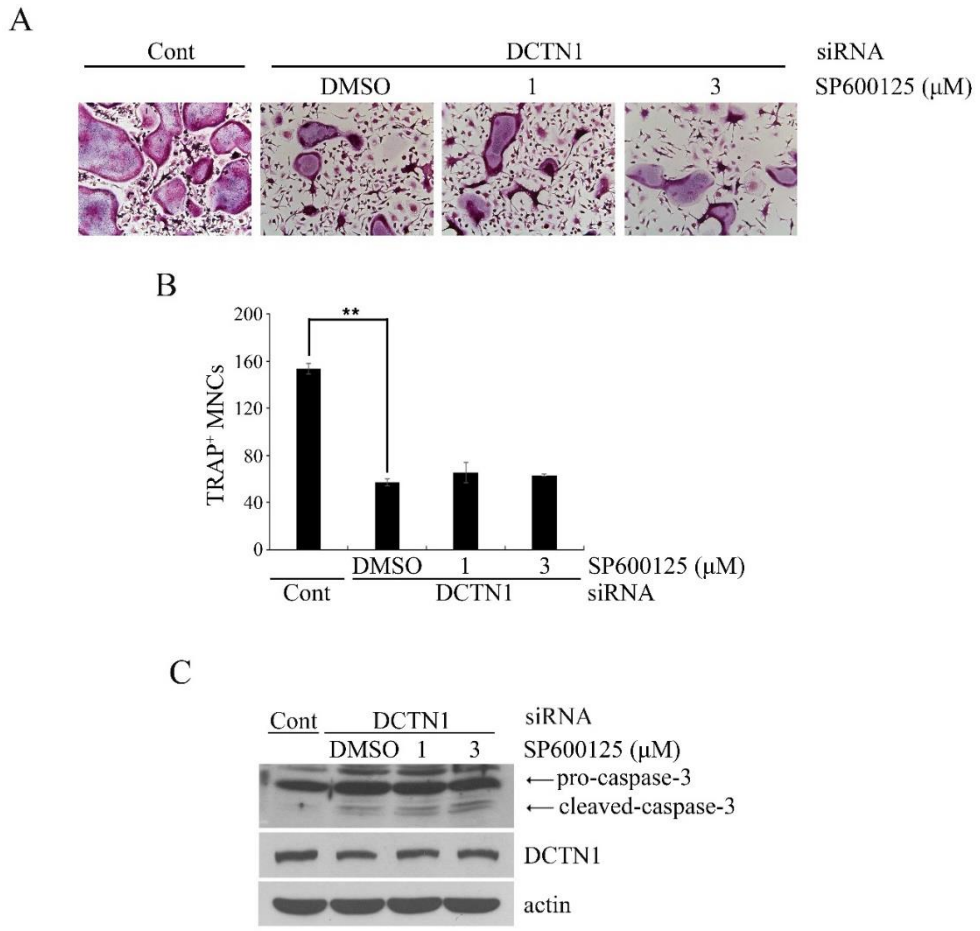

Figure 28. JNK inhibition did not rescue the defect of osteoclastogenesis.

(A) BMMs were transfected with control or DCTN1 siRNA for 24 hr. Cells were cultured in the presence of M-CSF (30 ng/ml) and RANKL (200 ng/ml) for 4 days with or without SP600125 during the first 48 hr for the indicated dose. (B) TRAP-positive multinucleated cells were counted. (C) BMMs were transfected

with control or DCTN1 siRNA for 24 hr. Cells were cultured in the presence of M-CSF (30 ng/ml) and RANKL (200 ng/ml) for 48 hr with or without SP600125. Caspase-3 and DCTN1 were detected by Western blotting. *, $p < 0.005$ as compared to controls. Cont, control siRNA; DCTN1, DCTN1 siRNA.

III.8. DCTN1 knockdown reduced osteoclastogenesis in vivo

Next, I examined whether the effect of DCTN1 siRNA on bone resorption could be verified in vivo. Control or DCTN1 siRNA oligonucleotides were injected into mice calvariae. Then, PBS- or RANKL-soaked collagen sponges were implanted. After 7 days of transplantation, the whole calvariae were stained for TRAP activity and subjected to μCT analysis. DCTN1 siRNA-injected mice showed reduced TRAP-positive area (Fig. 29, upper panel). In accordance with this result, μCT analysis of the calvariae showed reduced bone resorption in DCTN1 siRNA-injected mice (Fig. 29, lower panel). The mRNA expression of DCTN1 was efficiently inhibited by siRNA injection (Fig. 30). The mRNA levels of NFATc1 and TRAP were also decreased by DCTN1 knockdown (Fig. 30). For histological analysis, decalcified mice calvariae sections were stained for TRAP activity. The number of $TRAP^{+}$-cells was decreased in DCTN1 siRNA-injected calvariae (Fig. 31A). I found that DCTN1 knockdown decreased the OC number per bone perimeter (N.Oc/B.Pm) and the OC surface per bone surface (Oc.S/BS) as well as eroded surface per bone surface (ES/BS) in DCTN1 siRNA-injected calvariae (Fig. 31B). To verify whether DCTN1 siRNA injection on calvariae has an apoptotic effect, TUNEL assay was performed on calvariae sections. I found that the number of apoptotic OC precursor cells was increased (Fig. 32). Taken together, these results suggest that DCTN1 might have an essential role in the

prevention of RANKL-induced bone loss in vivo.

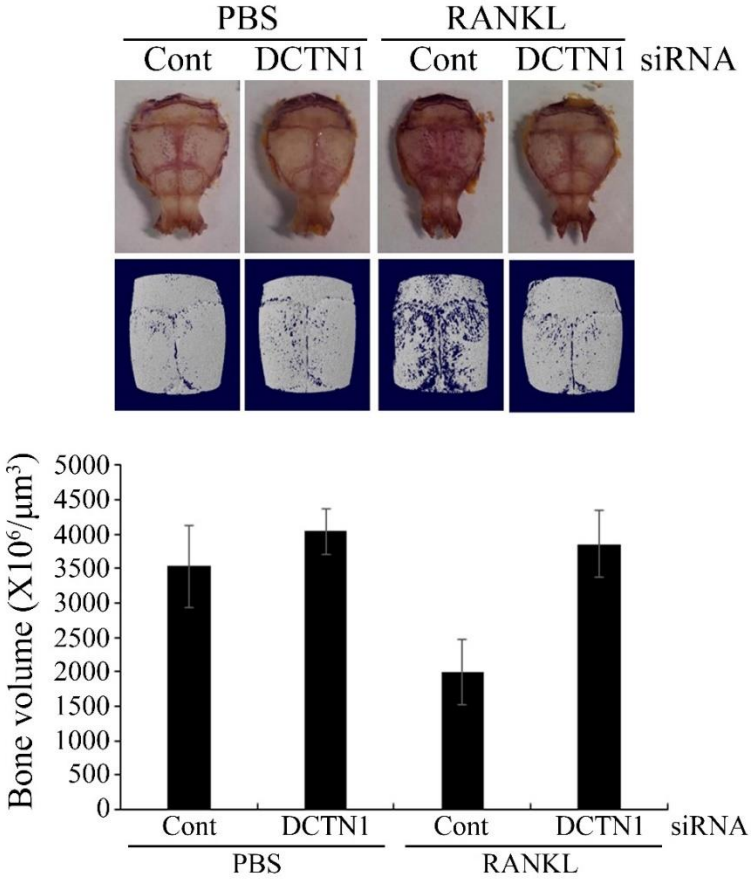

Figure 29. In vivo DCTN1 knockdown reduced osteoclastogenesis and bone volume.

Control or DCTN1 siRNA was injected onto calvariae of 5-week-old female mice, followed by implantation of a collagen sheet soaked with PBS or RANKL. The mice were sacrificed at day 7. Mice calvariae were stained for TRAP (upper panel). Calvariae were subjected to μCT analysis. 3D-images are shown. The

bone volume of calvariae was analyzed with CTAN software. n = 5 per group. *, $p < 0.05$ as compared to PBS, **, $p < 0.005$ as compared to control. Cont, control siRNA; DCTN1, DCTN1 siRNA.

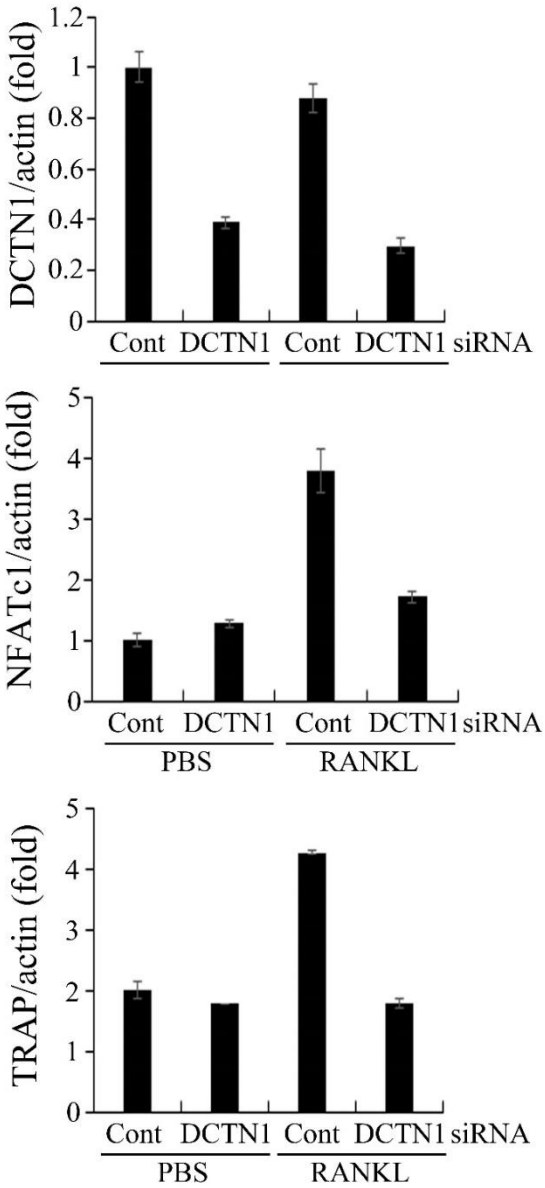

Figure 30. In vivo DCTN1 knockdown suppressed the induction of NFATc1 and TRAP.

The total mRNA extracts from mice calvariae tissues were used for analyzing the gene expression. The mRNA levels of DCTN1, NFATc1 and TRAP were analyzed by real-time PCR. *, $p < 0.05$; **, $p < 0.005$ as compared to control. Cont, control siRNA; DCTN1, DCTN1 siRNA.

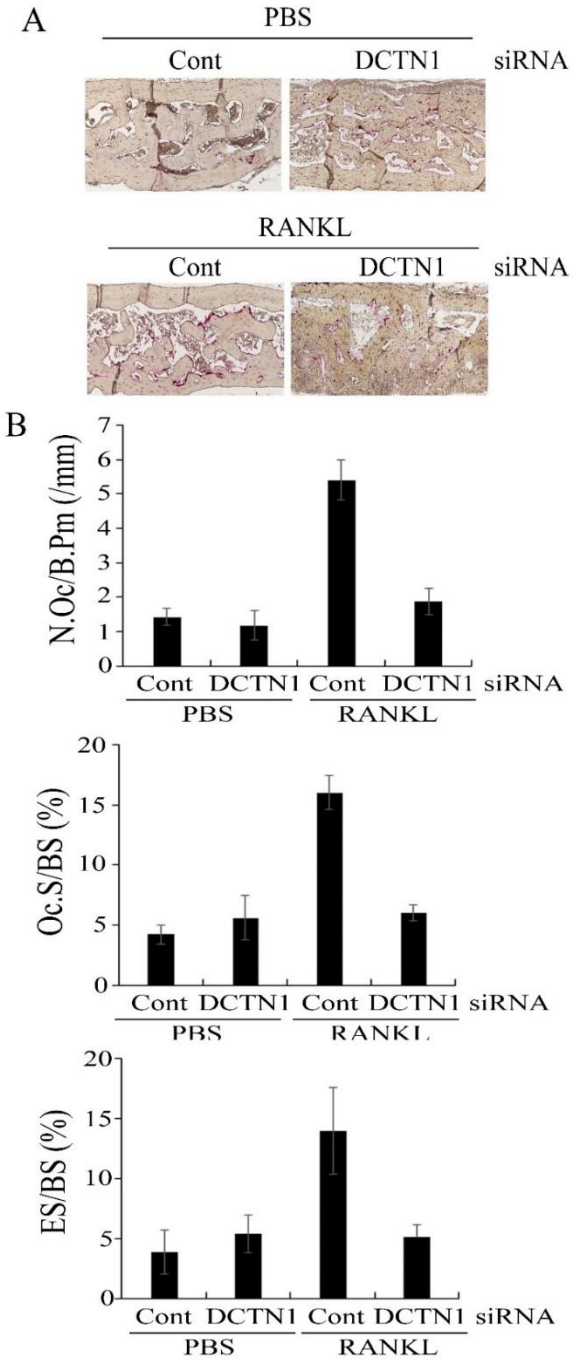
A
PBS
Cont
DCTN1
siRNA
RANKL
Cont
DCTN1
siRNA
B
N.Oc/B.Pm (/mm)
0
1
2
3
4
5
6
7
Cont DCTN1 Cont DCTN1 siRNA
PBS
RANKL
Oc.S/BS (%)
0
5
10
15
20
Cont DCTN1 Cont DCTN1 siRNA
PBS
RANKL
ES/BS (%)
0
5
10
15
20
Cont DCTN1 Cont DCTN1 siRNA
PBS
RANKL

Figure 31. Bone resorption was decreased in DCTN1-silenced mice calvariae. (A) Sections of calviarie were stained for TRAP activity. Representative images of stained sections are shown. (B) Quantitative analysis using the sections included the following parameters: OC number/bone perimeter (N.Oc/B.Pm); OC surface/bone surface (Oc.S/BS); eroded surface/bone surface (ES/BS). n = 5 per group. *, $p < 0.05$; **, $p < 0.005$ as compared to control. Cont, control siRNA; DCTN1, DCTN1 siRNA.

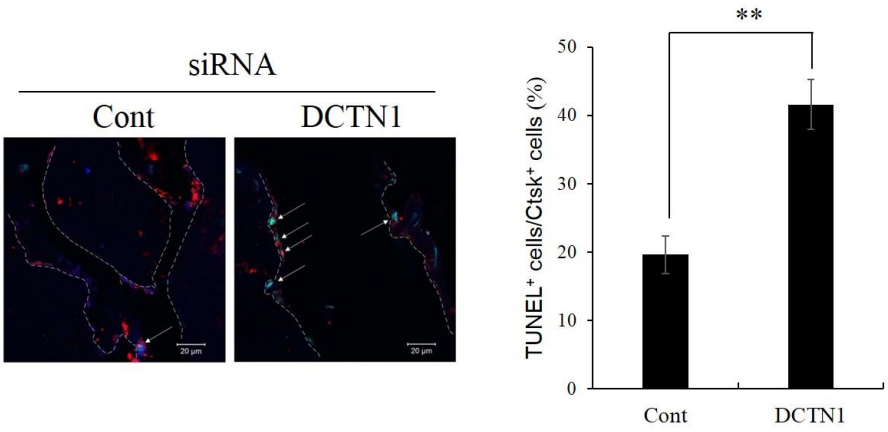

Figure 32. DCTN1 knockdown reduced the survival of OC precursor cells in vivo.

In vivo TUNEL assay was performed in sections of calvariae embedded in paraffin from control or DCTN1 siRNA-injected calvariae. White arrows indicate apoptotic OCs on bone surfaces. OCs were detected with anti-Ctsk (red), nuclei were stained with DAPI (blue). TUNEL-positive cells per Ctsk-positive cells were counted. **, $p < 0.005$ as compared to controls. Cont, control siRNA; DCTN1, DCTN1 siRNA.

III.9. Overexpression of DCTN1 interrupted osteoclastogenesis

It has been reported that excessive expression of some subunits of dynactin complex disrupts dynactin function (Schroer, 2004). I hypothesized that DCTN1 overexpression as well as DCTN1 knockdown may reduce osteoclastogenesis. BMMs infected with control or DCTN1-harboring retroviruses were cultured in the presence of M-CSF and RANKL. Like the result from silencing experiments, forced expression of DCTN1 significantly inhibited OC differentiation (Fig. 33A). The protein levels of both NFATc1 and c-Fos were also reduced by DCNT1 overexpression (Fig. 33B). I next investigated whether the forced expression of DCTN1 also suppressed the activation of Cdc42. I found that excessively expressed DCTN1 decreased the level of GTP-bound Cdc42 (Fig. 34). Next, I investigated effect of forced expression of DCTN1 on the apoptotic signaling. DCTN1-overexpressing BMMs were more susceptible to cell death and the expression of caspase-3 was increased (Fig. 35). However, cyclin D1 was unaltered by DCTN1 overexpression, like result from DCTN silencing experiments. It is likely that the activation of Cdc42 is essential pathway for DCTN1-mediated OC generation in the normal condition.

Based on the overexpression experiments, I hypothesize that the quantitative balancing of the DCTN1 expression is essential for normal OC differentiation, even though the induction of DCTN1 increased at early time upon RANKL

stimulation. To support this theory, I examined the dose-dependency effect on OC differentiation. The culture supernatant of DCTN1 overexpression-containing retroviruses at several dilutions with medium were added to BMMs for DCTN1 overexpression. Then, cells were further cultured in the presence of M-CSF and RANKL. As shown in Fig. 36, OC differentiation was inhibited in a manner dependent on viral dose. These results suggest that elaborate regulation of DCTN1 expression is important for normal osteoclastogenesis.

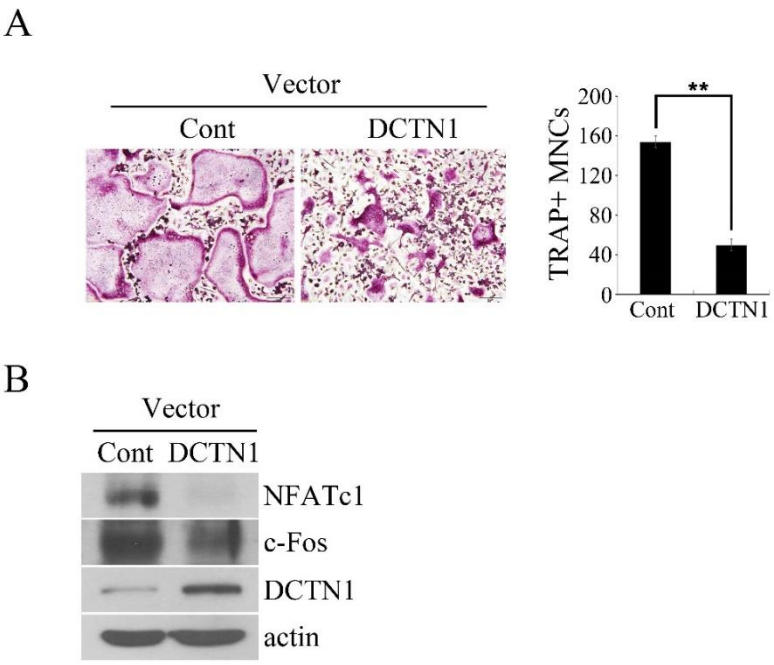

Figure 33. DCTN1 overexpression suppressed osteoclastogenesis.

(A) BMMs infected with supernatant-containing DCTN1-harboring retrovirus were cultured with M-CSF (30 ng/ml) and RANKL (200 ng/ml) for 4 days and stained for TRAP. TRAP-positive multinucleated cells were counted. (B) BMMs were infected with supernatant-containing DCTN1-harboring retrovirus. Cells were cultured with M-CSF (30 ng/ml) and RANKL (200 ng/ml) for 48 hr. The protein levels of NFATc1 and c-Fos were determined by Western blotting. **, $p < 0.005$ as compared to controls. Cont, control pMX vector; DCTN1, pMX vector containing DCTN1.

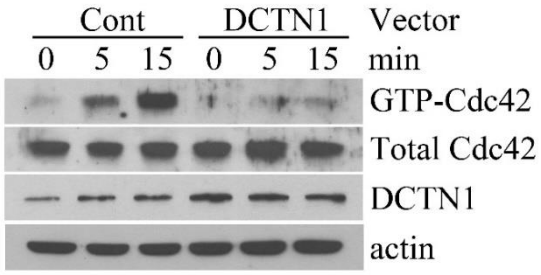

Figure 34. DCTN1 overexpression inhibited Cdc42 activation.

BMMs were infected with control or DCTN1-harboring retroviral supernatant. After serum starvation for 4 hr, cells were treated with RANKL (400 ng/ml) for the indicated times. The activated Cdc42 or Rac1 was precipitated using PBD-fusion GST bead. The levels of GTP-Cdc42 and DCTN1 were determined by Western blotting. Cont, control pMX vector; DCTN1, pMX vector containing DCTN1.

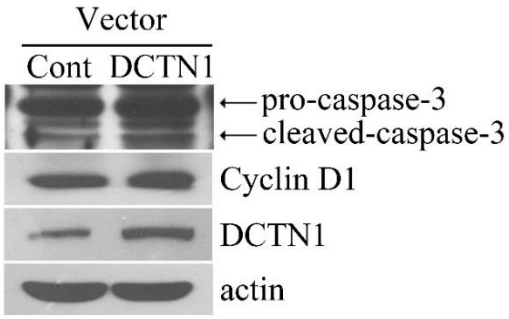

Figure 35. DCTN1 overexpression increased cleavage of caspase-3.

BMMs infected with control or DCTN1-harboring retroviral supernatant were cultured with M-CSF (30 ng/ml) and RANKL (200 ng/ml) for 48 hr. The protein levels of caspase-3, cyclin D1, and DCTN1 were determined by Western blotting. Cont, control pMX vector; DCTN1, pMX vector containing DCTN1.

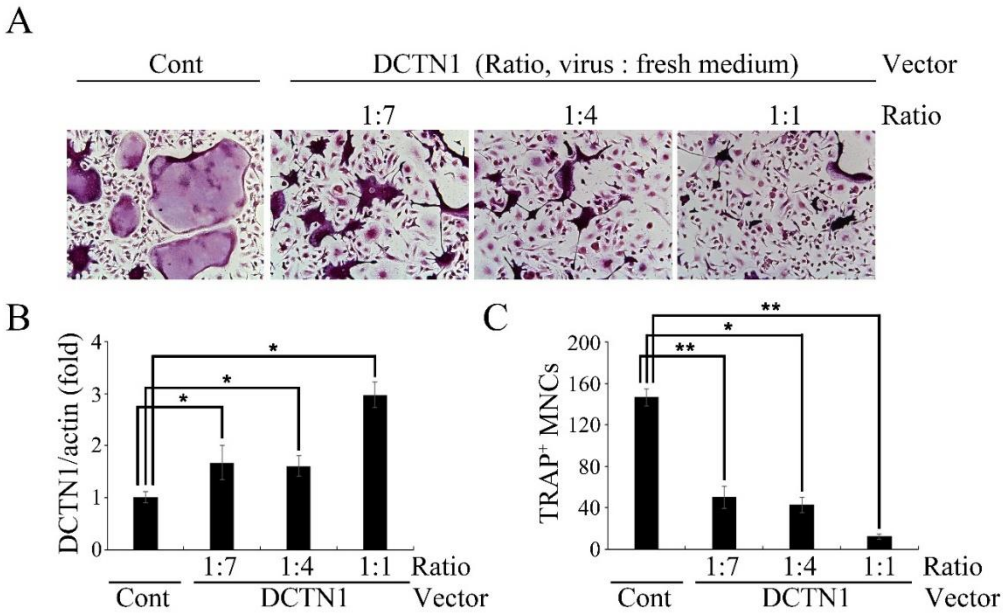

Figure 36. DCTN1 overexpression inhibited OC differentiation by retrovirus infection in a dose-dependent manner.

(A) BMMs infected with control or DCTN1-harboring retroviral supernatant diluted at for the indicated ratio (retrovirus supernatant : fresh culture medium). Cells were further cultured in the presence of M-CSF (30 ng/ml) and RANKL (200 ng/ml) for 4 days and stained for TRAP. (B) The level of DCTN1 mRNA was analyzed by real-time PCR. (C) TRAP-positive multinucleated cells were counted. *, $p < 0.05$; **, $p < 0.005$ as compared to controls. Cont, control pMX vector; DCTN1, pMX vector containing DCTN1.

IV. Discussion

Several reports indicated the association between motor proteins and bone. Osteoblast-specific Kif3a knockout mice showed a reduction in the mineral apposition rate (Qiu et al., 2012). Myosin IXB and myosin X have a critical role for podosome formation and resorption capacity of OC (McMichael et al., 2010; McMichael et al., 2014). Dynein light chain LC8 inhibited OC differentiation by regulating NF-κB (Kim et al., 2013b). DCTN1 has a central role in the dynactin complex for dynein motor. Our results newly obtained in this study indicate a link between DCTN1 and osteoclastogenesis, which is summarized in Fig. 37.

The level of DCTN1 was increased at early phase by RANKL and sustained at a constant level until OC maturation. DCTN1 knockdown inhibited OC differentiation through Cdc42 inactivation, which attributed to reduction of both NFATc1 and c-Fos expression. The small GTPase protein family has been shown to be involved in the regulation proliferation, apoptosis, and polarization of cytoskeleton structure (Erickson and Cerione, 2001; Marques et al., 2008). Cdc42, a small GTPase protein, has also been implicated in the regulation of cell survival and cytoskeleton (Erickson and Cerione, 2001). Cdc42 helps tumor survival against cytotoxic T-lymphocyte-mediated apoptosis through MAPK pathway and stabilization of Bcl-2 (Marques et al., 2008). The polarization of both actin and

microtubules in T-cells, when contacted with antigen-presenting cells, was regulated by Cdc42 (Stowers et al., 1995). In migrating cells, the microtubule-organizing center (MTOC) polarize to the leading edge (Gotlieb et al., 1981). A previous report indicated that Cdc42, cooperating with dynein/dynactin complex, regulated the MTOC reorientation (Palazzo et al., 2001). However, it has been unclear whether the DCTN1 is involved in the Cdc42 activation. In the present study, I revealed that DCTN1 exerts its effect by regulating the activation of Cdc42 (Fig. 13A). In a previous report, Cdc42 depletion increased bone volume and protected ovariectomy-induced bone loss. Cdc42-deficient OCs decreased resorption capacity and impaired M-CSF or RANKL-mediated signaling events. (Ito et al., 2010). The reduction of GTP-bound Cdc42 level by DCTN1 silencing affected intracellular signaling pathways such as ERK1/2, p38, JNK, and Akt, which is essential for osteoclastogenesis and inhibited the induction of NFATc1 (Figs. 10 and 12). These observations were verified by retroviral infection of constitutively active Cdc42. The overexpression of constitutively active Cdc42 in DCTN1 silenced BMMs restored OC differentiation, MAPK and Akt signaling, and the induction of NFATc1 and c-Fos (Figs. 15 and 16).

Although ERK1/2 and p38 were downregulated, the phosphorylation of JNK was increased in DCTN1-silenced BMMs (Fig. 12). A previous report showed that RANKL-mediated JNK activation increased the susceptibility to apoptosis

and disrupted normal OC generation in RelA$^{-/-}$ mice (Vaira et al., 2008). Tissue-damage-induced cell death by external stimuli activates proliferation mechanism, simultaneously. In this context, the activation of JNK has a crucial role in both apoptosis and compensatory proliferation (Warner et al., 2010). I found that absence of DCTN1 accelerated OC precursor cell apoptosis (Fig. 24). I investigated whether the elevation in JNK activation reduces OC differentiation. However, JNK inhibition by SP600125 could not prevent apoptosis and inhibition of OC generation by DCTN1 silencing (Fig. 28). It is likely that the increase in JNK activation is compensatory mechanism to cover the impairment of MAPK cascasdes.

Activated Cdc42, interacting with its effector molecules, regulates diverse cellular events (Melendez et al., 2011). p21-activated kinases (PAKs) serve as a downstream molecule of Cdc42 signaling. Activated Cdc42, bind to PBD domain in PAKs, induces autophosphorylation which activates PAKs (Knaus and Bokoch, 1998). PAKs have been involved in multiple cellular processes including MAPK signaling, cell survival, and cytoskeleton reorganization (Phee et al., 2014; Rane and Minden, 2014). PAK2 siRNA transfected BMMs showed decreased OC differentiation and disruption of MAPK signaling cascades by RANKL (Figs. 20 and 21). These results indicate that effect of DCTN1-mediated Cdc42 activation on MAPK pathways appears to be achieved through the PAK2 activation.

However, these results are in conflict with a recent study that PAK4 is predominantly expressed and has a major role in OC differentiation (Choi et al., 2015). In this study, they used BMMs from 5-week-old ICR male mice. It is likely that the expression pattern of PAK family is sex-dependent.

Several subunits of dynactin complex prevent dynactin function when they are excessively expressed. The overexpressed DCTN2, which impairs the interaction between dynein and dynactin and disrupts dynactin structure, is broadly used as a strategy to block the dynein function (Kardon and Vale, 2009; Raaijmakers et al., 2013). Other subunits, like Arp11 or p62 also prevent the dynactin binding with its cellular targets (Schroer, 2004). Arp1 overexpression disrupted perinuclear localization of Golgi in PtK2 cells (Holleran et al., 1996). It suggests that the balance of each subunit is important for dynactin function. The excessive DCTN1 expression significantly inhibited OC differentiation and the activation of Cdc42 by RANKL (Figs. 31 and 32). Particulary, slight alteration in DCTN1 expression was sufficient to block OC generation (Fig. 36). Although the expression of DCTN1 increased at early phase and sustained OC differentiation, these results lead to a supposition that sustaining DCTN1 at a proper level is essential for normal osteoclastogenesis. However, DCTN1 overexpression did not disrupt the interaction between dynein and dynactin in Cos-7 cells and influence on dynein function was unclear (Quintyne et al., 1999; Waterman-

Storer et al., 1995). I could not determine whether overexpressed DCTN1 might have altered the interaction between dynein and dynactin or among the components of dynactin complex itself in this research.

Ng et al reported evidence for the role of DCTN2 in OCs, mainly focused on OC function. The DCTN2 overexpression decreased OC function through inhibition of cathepsin K secretion. Although, they also showed inhibition of OC differentiation, some results were inconsistent with my experimental results (Ng et al., 2013). First, the signaling events including MAPK activation were unalterd by DCTN2 overexpression in the study by Ng et al. However, the phosphorylation of MAPK and Akt was significantly changed in my experiments (Fig. 12). Second, the level of Src protein itself was decreased by DCTN2 overexpression. Src kinase acts as an upstream effector for the Cdc42 activation (Fukuhara et al., 2004). However, the level of phosphorylated Src was modestly increased by DCTN1 knockdown (Fig. 17). According to these results, it is likely that each subunit of dynactin complex may lead to different cellular events in OC differentiation, like subunits of V-ATPase, such as a3, d2, and Ac45, do (Qin et al., 2012). Dynactin subunits collaborate with its diverse binding partners (Eschbach and Dupuis, 2011; Liang et al., 2004; Schroer, 2004). For example, DCTN2 directly interacted calmodulin, the cellular function of their binding was unveiled, however (Yue et al., 2000). In MCF-7 cells, ERα interacts with DCTN1.

Estrogen induces the recruitment of DCTN1 at the promoter region of estrogen-responsive gene. Knockdown of DCTN1 reduces estrogen-dependent transcription (Lee et al., 2009). Dynein light chain is also found in the nucleus. It has been shown to bind ERα, to promote transcription of ERα target gene (Rayala et al., 2005). These results indicate that each subunit of dynactin complex not as a component of adaptor have unique function. Alternatively, it is likely that the different cellular signaling events is raised, depending on which binding partners cooperate with dynactin subunits. Further studies are required to define the effect of each subunit during OC differentiation.

It has been reported that DCTN1 was phosphorylated exclusively on serine by TPA or okadaic acid stimulation. This phosphorylation positively regulated DCTN1 function. (Farshori and Holzbaur, 1997). Reboutier et al showed that DCTN1, which is phosphorylated on serine 19 by aurora kinase A, regulated central spindle assembly during anaphase (Reboutier et al., 2013). Indeed, I found that RANKL increases the induction of aurora kinase A in OC precursor cells. Aurora kinase A specific inhibitor sufficiently inhibited serine phosphorylation of DCTN1 (data not shown). There is another possibility. RANKL-RANK signaling pathways may regulate DCTN1 activation. ERK1/2 pathway induces the phosphorylation of dynein intermediate chain for dynein-mediated axonal transport in rat pheochromocytoma (PC12) cells (Mitchell et al., 2012). In rat

primary cortical neuron cells, huntingtin protein, which is phosphorylated by Akt, promotes kinesin-1/dynactin complex-dependent anterograde transport. However, kinesin-1 is dissociated from microtubule when huntingtin is not phosphorylated. In this condition, retrograde transport is increased (Colin et al., 2008). Since MAPK and Akt pathways is important during osteoclastogenesis, RANKL-induced MAPK or Akt activation may lead to DCTN1 phosphorylation in early phase of osteoclastogenesis.

The phosphorylation of DCTN1 promotes cargo transportation including signaling molecules. Many protein kinases have been shown to bind to or be localized on microtubules. (Gundersen and Cook, 1999). MAPK family members, such as ERK1/2, p38, and JNK, were observed in association with microtubules (Gundersen and Cook, 1999; Reszka et al., 1995). Activated JNK by mixed-lineage kinases (MLKs), MAPK kinase kinase-like protein, was associated with microtubules in fibroblasts (Nagata et al., 1998). DCTN1 interacts with MKK3/6. DCTN1 knockdown reduced the phosphorylation of MKK3/6 and p38 MAPKs. MKK3/6, interacts with DCTN1, binds to microtubules. The activated DCTN1 can be participate this event for targeting signaling molecules to microtubules to activate signaling molecules. Microtubules depolymerization by nocodazole or colchicine inhibits the activation of both MKK3/6 and p38 (Cheung et al., 2004). Localization of Akt to microtubules sustains its phosphorylation. The

stabilization of microtubules is also important for Akt signaling. Recruitment of Akt to microtubules is mediated by DCTN1. Akt inactivation by microtubule disruption contributes to accelerated cell death (Jo et al., 2014). The effect of drugs that depolymerize microtubules on signaling molecules suggests that microtubules are likely to be critical to the regulation of signal transduction. Activated Rac1 also binds directly to tubulin in vitro and co-localized with microtubule structure in Swiss 3T3 cells (Best et al., 1996). Vav1, a GEF for Rac and Rho, was shown to interacte with tubulin in T cells (Huby et al., 1995). GTP-bound Cdc42 also associated with microtubules through CLIP-170 (Fukata et al., 2002). These results indicate that microtubules may act as a scaffold for signaling molecules during OC differentiation. In this context, DCTN1 can target the activated Cdc42 and ERK1/2, p38, JNK, and Akt to the microtubule structure to build signaling platform.

In summary, this study unveils an important role of DCTN1 in OC differentiation. The constant presence of DCTN1 at an optimal level is indispensable for osteoclastogenesis. Additionally, I uncovered the mechanism how DCTN1 regulates OC differentiation for the first time. RANKL-dependent activation of dynactin complex modulates Cdc42/PAK2 axis that regulates the induction of NFATc1 and cell survival during osteoclastogenesis.

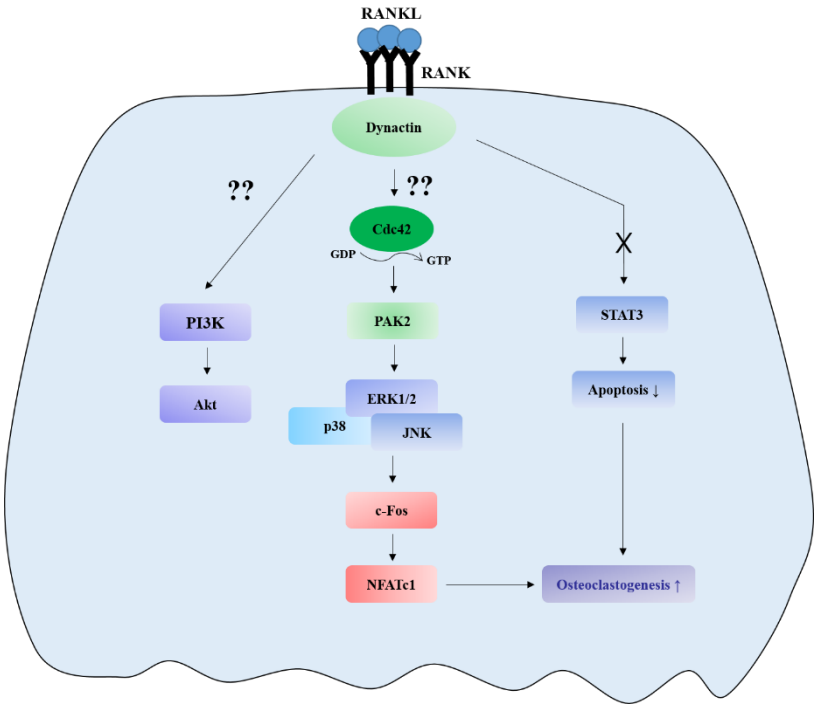

Figure 37. Schematic model of the proposed mechanism by which DCTN1 regulates osteoclastogenesis.

RANKL activates dynactin through unknown mechanism that increases GTP-bound Cdc42 (the activated form) via unknown mechanisms. The active Cdc42 phosphorylates PAK2, that induces MAPK and Akt signaling. Ultimately, a chain of signaling cascades activates induction of NFATc1. Simultaneously, the activation of dynactin complex decreases apoptosis of osteoclast precursor cells via the inhibition of STAT3.

V. References

Asagiri, M., and H. Takayanagi. 2007. The molecular understanding of osteoclast differentiation. *Bone*. 40:251-264.

Best, A., S. Ahmed, R. Kozma, and L. Lim. 1996. The Ras-related GTPase Rac1 binds tubulin. *J. Biol. Chem.* 271:3756-3762.

Boyle, W.J., W.S. Simonet, and D.L. Lacey. 2003. Osteoclast differentiation and activation. *Nature*. 423:337-342.

Chang, E.J., J. Ha, F. Oerlemans, Y.J. Lee, S.W. Lee, J. Ryu, H.J. Kim, Y. Lee, H.M. Kim, J.Y. Choi, J.Y. Kim, C.S. Shin, Y.K. Pak, S. Tanaka, B. Wieringa, Z.H. Lee, and H.H. Kim. 2008. Brain-type creatine kinase has a crucial role in osteoclast-mediated bone resorption. *Nat. Med.* 14:966-972.

Chen, T.Y., J.S. Syu, T.Y. Han, H.L. Cheng, F.I. Lu, and C.Y. Wang. 2015. Cell cycle-dependent localization of dynactin subunit p150 Glued at centrosome. *J. Cell. Biochem.* 116:2049-2060.

Cheung, P.Y., Y. Zhang, J. Long, S. Lin, M. Zhang, Y. Jiang, and Z. Wu. 2004. p150(Glued), Dynein, and microtubules are specifically required for activation of MKK3/6 and p38 MAPKs. *J. Biol. Chem.* 279:45308-45311.

Choi, S.W., J.T. Yeon, B.J. Ryu, K.J. Kim, S.H. Moon, H. Lee, M.S. Lee, S.Y. Lee, J.C. Heo, S.J. Park, and S.H. Kim. 2015. Repositioning potential of

PAK4 to osteoclastic bone resorption. *J. Bone Miner. Res.* 30:1494-1507.

Colin, E., D. Zala, G. Liot, H. Rangone, M. Borrell-Pages, X.J. Li, F. Saudou, and S. Humbert. 2008. Huntingtin phosphorylation acts as a molecular switch for anterograde/retrograde transport in neurons. *EMBO J.* 27:2124-2134.

De Vos, K.J., A.J. Grierson, S. Ackerley, and C.C. Miller. 2008. Role of axonal transport in neurodegenerative diseases. *Annu. Rev. Neurosci.* 31:151-173.

Dummler, B., K. Ohshiro, R. Kumar, and J. Field. 2009. Pak protein kinases and their role in cancer. *Cancer Metastasis Rev.* 28:51-63.

Erickson, J.W., and R.A. Cerione. 2001. Multiple roles for Cdc42 in cell regulation. *Curr. Opin. Cell Biol.* 13:153-157.

Eschbach, J., and L. Dupuis. 2011. Cytoplasmic dynein in neurodegeneration. *Pharmacol. Ther.* 130:348-363.

Farshori, P., and E.L. Holzbaur. 1997. Dynactin phosphorylation is modulated in response to cellular effectors. *Biochem. Biophys. Res. Commun.* 232:810-816.

Fukata, M., T. Watanabe, J. Noritake, M. Nakagawa, M. Yamaga, S. Kuroda, Y. Matsuura, A. Iwamatsu, F. Perez, and K. Kaibuchi. 2002. Rac1 and Cdc42 capture microtubules through IQGAP1 and CLIP-170. *Cell*. 109:873-885.

Fukuhara, T., K. Shimizu, T. Kawakatsu, T. Fukuyama, Y. Minami, T. Honda, T.

Hoshino, T. Yamada, H. Ogita, M. Okada, and Y. Takai. 2004. Activation of Cdc42 by trans interactions of the cell adhesion molecules nectins through c-Src and Cdc42-GEF FRG. *J. Cell Biol.* 166:393-405.

Georgess, D., M. Mazzorana, J. Terrado, C. Delprat, C. Chamot, R.M. Guasch, I. Perez-Roger, P. Jurdic, and I. Machuca-Gayet. 2014. Comparative transcriptomics reveals RhoE as a novel regulator of actin dynamics in bone-resorbing osteoclasts. *Mol. Biol. Cell*. 25:380-396.

Gotlieb, A.I., L.M. May, L. Subrahmanyan, and V.I. Kalnins. 1981. Distribution of microtubule organizing centers in migrating sheets of endothelial cells. *J. Cell Biol.* 91:589-594.

Grigoriadis, A.E., Z.Q. Wang, M.G. Cecchini, W. Hofstetter, R. Felix, H.A. Fleisch, and E.F. Wagner. 1994. c-Fos: a key regulator of osteoclast-macrophage lineage determination and bone remodeling. *Science*. 266:443-448.

Guerini, D. 1997. Calcineurin: not just a simple protein phosphatase. *Biochem. Biophys. Res. Commun.* 235:271-275.

Gundersen, G.G., and T.A. Cook. 1999. Microtubules and signal transduction. *Curr. Opin. Cell Biol.* 11:81-94.

Habermann, A., T.A. Schroer, G. Griffiths, and J.K. Burkhardt. 2001. Immunolocalization of cytoplasmic dynein and dynactin subunits in

cultured macrophages: enrichment on early endocytic organelles. *J. Cell Sci.* 114:229-240.

Hogan, P.G., L. Chen, J. Nardone, and A. Rao. 2003. Transcriptional regulation by calcium, calcineurin, and NFAT. *Genes Dev.* 17:2205-2232.

Holleran, E.A., M.K. Tokito, S. Karki, and E.L. Holzbaur. 1996. Centractin (ARP1) associates with spectrin revealing a potential mechanism to link dynactin to intracellular organelles. *J. Cell Biol.* 135:1815-1829.

Howell, B.J., B.F. McEwen, J.C. Canman, D.B. Hoffman, E.M. Farrar, C.L. Rieder, and E.D. Salmon. 2001. Cytoplasmic dynein/dynactin drives kinetochore protein transport to the spindle poles and has a role in mitotic spindle checkpoint inactivation. *J. Cell Biol.* 155:1159-1172.

Huang, H., E.J. Chang, J. Ryu, Z.H. Lee, Y. Lee, and H.H. Kim. 2006. Induction of c-Fos and NFATc1 during RANKL-stimulated osteoclast differentiation is mediated by the p38 signaling pathway. *Biochem. Biophys. Res. Commun.* 351:99-105.

Huby, R.D., G.W. Carlile, and S.C. Ley. 1995. Interactions between the protein-tyrosine kinase ZAP-70, the proto-oncoprotein Vav, and tubulin in Jurkat T cells. *J. Biol. Chem.* 270:30241-30244.

Hunter, T. 1987. A tail of two src's: mutatis mutandis. *Cell*. 49:1-4.

Ikeda, F., R. Nishimura, T. Matsubara, S. Tanaka, J. Inoue, S.V. Reddy, K. Hata,

K. Yamashita, T. Hiraga, T. Watanabe, T. Kukita, K. Yoshioka, A. Rao, and T. Yoneda. 2004. Critical roles of c-Jun signaling in regulation of NFAT family and RANKL-regulated osteoclast differentiation. *J. Clin. Invest.* 114:475-484.

Ikenaka, K., K. Kawai, M. Katsuno, Z. Huang, Y.M. Jiang, Y. Iguchi, K. Kobayashi, T. Kimata, M. Waza, F. Tanaka, I. Mori, and G. Sobue. 2013. Dnc-1/dynactin 1 knockdown disrupts transport of autophagosomes and induces motor neuron degeneration. *PLoS One*. 8:e54511.

Ito, Y., S.L. Teitelbaum, W. Zou, Y. Zheng, J.F. Johnson, J. Chappel, F.P. Ross, and H. Zhao. 2010. Cdc42 regulates bone modeling and remodeling in mice by modulating RANKL/M-CSF signaling and osteoclast polarization. *J. Clin. Invest.* 120:1981-1993.

Jaffe, A.B., and A. Hall. 2005. Rho GTPases: biochemistry and biology. *Annu. Rev. Cell Dev. Biol.* 21:247-269.

Jo, H., F. Loison, and H.R. Luo. 2014. Microtubule dynamics regulates Akt signaling via dynactin p150. *Cell. Signal.* 26:1707-1716.

Johnson, D.I., and J.R. Pringle. 1990. Molecular characterization of CDC42, a Saccharomyces cerevisiae gene involved in the development of cell polarity. *J. Cell Biol.* 111:143-152.

Kardon, J.R., and R.D. Vale. 2009. Regulators of the cytoplasmic dynein motor.

Nat. Rev. Mol. Cell Biol. 10:854-865.

Karki, S., and E.L. Holzbaur. 1999. Cytoplasmic dynein and dynactin in cell division and intracellular transport. *Curr. Opin. Cell Biol.* 11:45-53.

Kim, D.J., L.A. Martinez-Lemus, and G.E. Davis. 2013. EB1, p150Glued, and Clasp1 control endothelial tubulogenesis through microtubule assembly, acetylation, and apical polarization. *Blood*. 121:3521-3530.

Kim, H., S. Hyeon, H. Kim, Y. Yang, J.Y. Huh, D.R. Park, H. Lee, D.H. Seo, H.S. Kim, S.Y. Lee, and W. Jeong. 2013. Dynein light chain LC8 inhibits osteoclast differentiation and prevents bone loss in mice. *J. Immunol.* 190:1312-1318.

King, S.J., and T.A. Schroer. 2000. Dynactin increases the processivity of the cytoplasmic dynein motor. *Nat. Cell Biol.* 2:20-24.

Klee, C.B., H. Ren, and X. Wang. 1998. Regulation of the calmodulin-stimulated protein phosphatase, calcineurin. *J. Biol. Chem.* 273:13367-13370.

Knaus, U.G., and G.M. Bokoch. 1998. The p21Rac/Cdc42-activated kinases (PAKs). *Int. J. Biochem. Cell Biol.* 30:857-862.

Knaus, U.G., S. Morris, H.J. Dong, J. Chernoff, and G.M. Bokoch. 1995. Regulation of human leukocyte p21-activated kinases through G protein--coupled receptors. *Science*. 269:221-223.

Kong, Y.Y., U. Feige, I. Sarosi, B. Bolon, A. Tafuri, S. Morony, C. Capparelli, J.

Li, R. Elliott, S. McCabe, T. Wong, G. Campagnuolo, E. Moran, E.R. Bogoch, G. Van, L.T. Nguyen, P.S. Ohashi, D.L. Lacey, E. Fish, W.J. Boyle, and J.M. Penninger. 1999. Activated T cells regulate bone loss and joint destruction in adjuvant arthritis through osteoprotegerin ligand. *Nature*. 402:304-309.

Kunoh, T., T. Noda, K. Koseki, M. Sekigawa, M. Takagi, K. Shin-ya, N. Goshima, S. Iemura, T. Natsume, S. Wada, Y. Mukai, S. Ohta, R. Sasaki, and T. Mizukami. 2010. A novel human dynactin-associated protein, dynAP, promotes activation of Akt, and ergosterol-related compounds induce dynAP-dependent apoptosis of human cancer cells. *Mol. Cancer Ther.* 9:2934-2942.

Lee, J.H., H. Jin, H.E. Shim, H.N. Kim, H. Ha, and Z.H. Lee. 2010. Epigallocatechin-3-gallate inhibits osteoclastogenesis by down-regulating c-Fos expression and suppressing the nuclear factor-kappaB signal. *Mol. Pharmacol.* 77:17-25.

Lee, N.K., H.K. Choi, D.K. Kim, and S.Y. Lee. 2006. Rac1 GTPase regulates osteoclast differentiation through TRANCE-induced NF-kappa B activation. *Mol. Cell. Biochem.* 281:55-61.

Lee, S.J., C. Chae, and M.M. Wang. 2009. p150Glued modifies nuclear estrogen receptor function. *Mol. Endocrinol.* 23:620-629.

Lee, Z.H., and H.H. Kim. 2003. Signal transduction by receptor activator of nuclear factor kappa B in osteoclasts. *Biochem. Biophys. Res. Commun.* 305:211-214.

Levy, J.R., and E.L. Holzbaur. 2006. Cytoplasmic dynein/dynactin function and dysfunction in motor neurons. *Int. J. Dev. Neurosci.* 24:103-111.

Levy, J.R., C.J. Sumner, J.P. Caviston, M.K. Tokito, S. Ranganathan, L.A. Ligon, K.E. Wallace, B.H. LaMonte, G.G. Harmison, I. Puls, K.H. Fischbeck, and E.L. Holzbaur. 2006. A motor neuron disease-associated mutation in p150Glued perturbs dynactin function and induces protein aggregation. *J. Cell Biol.* 172:733-745.

Li, K., L. Yang, C. Zhang, Y. Niu, W. Li, and J.J. Liu. 2014. HPS6 interacts with dynactin p150Glued to mediate retrograde trafficking and maturation of lysosomes. *J. Cell Sci.* 127:4574-4588.

Li, X., F. Liu, and F. Li. 2010. PAK as a therapeutic target in gastric cancer. *Expert Opin. Ther. Targets*. 14:419-433.

Liang, Y., W. Yu, Y. Li, Z. Yang, X. Yan, Q. Huang, and X. Zhu. 2004. Nudel functions in membrane traffic mainly through association with Lis1 and cytoplasmic dynein. *J. Cell Biol.* 164:557-566.

Marques, C.A., P.S. Hahnel, C. Wolfel, S. Thaler, C. Huber, M. Theobald, and M. Schuler. 2008. An immune escape screen reveals Cdc42 as regulator of

cancer susceptibility to lymphocyte-mediated tumor suppression. *Blood*. 111:1413-1419.

McMichael, B.K., R.E. Cheney, and B.S. Lee. 2010. Myosin X regulates sealing zone patterning in osteoclasts through linkage of podosomes and microtubules. *J. Biol. Chem.* 285:9506-9515.

McMichael, B.K., K.F. Scherer, N.C. Franklin, and B.S. Lee. 2014. The RhoGAP activity of myosin IXB is critical for osteoclast podosome patterning, motility, and resorptive capacity. *PLoS One*. 9:e87402.

Melendez, J., M. Grogg, and Y. Zheng. 2011. Signaling role of Cdc42 in regulating mammalian physiology. *J. Biol. Chem.* 286:2375-2381.

Mitchell, D.J., K.R. Blasier, E.D. Jeffery, M.W. Ross, A.K. Pullikuth, D. Suo, J. Park, W.R. Smiley, K.W. Lo, J. Shabanowitz, C.D. Deppmann, J.C. Trinidad, D.F. Hunt, A.D. Catling, and K.K. Pfister. 2012. Trk activation of the ERK1/2 kinase pathway stimulates intermediate chain phosphorylation and recruits cytoplasmic dynein to signaling endosomes for retrograde axonal transport. *J. Neurosci.* 32:15495-15510.

Miyazaki, T., A. Sanjay, L. Neff, S. Tanaka, W.C. Horne, and R. Baron. 2004. Src kinase activity is essential for osteoclast function. *J. Biol. Chem.* 279:17660-17666.

Mundy, G.R. 2002. Metastasis to bone: causes, consequences and therapeutic

opportunities. *Nat. Rev. Cancer*. 2:584-593.

Nagata, K., A. Puls, C. Futter, P. Aspenstrom, E. Schaefer, T. Nakata, N. Hirokawa, and A. Hall. 1998. The MAP kinase kinase kinase MLK2 co-localizes with activated JNK along microtubules and associates with kinesin superfamily motor KIF3. *EMBO J.* 17:149-158.

Nakashima, T., and H. Takayanagi. 2011. New regulation mechanisms of osteoclast differentiation. *Ann. N. Y. Acad. Sci.* 1240:E13-18.

Negishi-Koga, T., and H. Takayanagi. 2009. Ca2+-NFATc1 signaling is an essential axis of osteoclast differentiation. *Immunol. Rev.* 231:241-256.

Ng, P.Y., T.S. Cheng, H. Zhao, S. Ye, E. Sm Ang, E.C. Khor, H.T. Feng, J. Xu, M.H. Zheng, and N.J. Pavlos. 2013. Disruption of the dynein-dynactin complex unveils motor-specific functions in osteoclast formation and bone resorption. *J. Bone Miner. Res.* 28:119-134.

Nicholls, J.J., M.J. Brassill, G.R. Williams, and J.H. Bassett. 2012. The skeletal consequences of thyrotoxicosis. *J. Endocrinol.* 213:209-221.

Palazzo, A.F., H.L. Joseph, Y.J. Chen, D.L. Dujardin, A.S. Alberts, K.K. Pfister, R.B. Vallee, and G.G. Gundersen. 2001. Cdc42, dynein, and dynactin regulate MTOC reorientation independent of Rho-regulated microtubule stabilization. *Curr. Biol.* 11:1536-1541.

Paschal, B.M., H.S. Shpetner, and R.B. Vallee. 1987. MAP 1C is a microtubule-

activated ATPase which translocates microtubules in vitro and has dynein-like properties. *J. Cell Biol.* 105:1273-1282.

Phee, H., B.B. Au-Yeung, O. Pryshchep, K.L. O'Hagan, S.G. Fairbairn, M. Radu, R. Kosoff, M. Mollenauer, D. Cheng, J. Chernoff, and A. Weiss. 2014. PAK2 is required for actin cytoskeleton remodeling, TCR signaling, and normal thymocyte development and maturation. *Elife*. 3:e02270.

Qin, A., T.S. Cheng, N.J. Pavlos, Z. Lin, K.R. Dai, and M.H. Zheng. 2012. V-ATPases in osteoclasts: structure, function and potential inhibitors of bone resorption. *Int. J. Biochem. Cell Biol.* 44:1422-1435.

Qiu, N., Z. Xiao, L. Cao, M.M. Buechel, V. David, E. Roan, and L.D. Quarles. 2012. Disruption of Kif3a in osteoblasts results in defective bone formation and osteopenia. *J. Cell Sci.* 125:1945-1957.

Quintyne, N.J., S.R. Gill, D.M. Eckley, C.L. Crego, D.A. Compton, and T.A. Schroer. 1999. Dynactin is required for microtubule anchoring at centrosomes. *J. Cell Biol.* 147:321-334.

Raaijmakers, J.A., M.E. Tanenbaum, and R.H. Medema. 2013. Systematic dissection of dynein regulators in mitosis. *J. Cell Biol.* 201:201-215.

Rane, C.K., and A. Minden. 2014. p21-activated kinases: structure, regulation, and functions. *Small GTPases*. 5.

Rayala, S.K., P. den Hollander, S. Balasenthil, Z. Yang, R.R. Broaddus, and R.

Kumar. 2005. Functional regulation of oestrogen receptor pathway by the dynein light chain 1. *EMBO reports*. 6:538-544.

Reboutier, D., M.B. Troadec, J.Y. Cremet, L. Chauvin, V. Guen, P. Salaun, and C. Prigent. 2013. Aurora A is involved in central spindle assembly through phosphorylation of Ser 19 in P150Glued. *J. Cell Biol.* 201:65-79.

Reszka, A.A., R. Seger, C.D. Diltz, E.G. Krebs, and E.H. Fischer. 1995. Association of mitogen-activated protein kinase with the microtubule cytoskeleton. *Proc. Natl. Acad. Sci. U. S. A.* 92:8881-8885.

Rodriguez-Gonzalez, A., T. Lin, A.K. Ikeda, T. Simms-Waldrip, C. Fu, and K.M. Sakamoto. 2008. Role of the aggresome pathway in cancer: targeting histone deacetylase 6-dependent protein degradation. *Cancer Res.* 68:2557-2560.

Sato, K., A. Suematsu, T. Nakashima, S. Takemoto-Kimura, K. Aoki, Y. Morishita, H. Asahara, K. Ohya, A. Yamaguchi, T. Takai, T. Kodama, T.A. Chatila, H. Bito, and H. Takayanagi. 2006. Regulation of osteoclast differentiation and function by the CaMK-CREB pathway. *Nat. Med.* 12:1410-1416.

Schroer, T.A. 2004. Dynactin. *Annu. Rev. Cell Dev. Biol.* 20:759-779.

Sells, M.A., U.G. Knaus, S. Bagrodia, D.M. Ambrose, G.M. Bokoch, and J. Chernoff. 1997. Human p21-activated kinase (Pak1) regulates actin

organization in mammalian cells. *Curr. Biol.* 7:202-210.

Sharp, D.J., G.C. Rogers, and J.M. Scholey. 2000. Cytoplasmic dynein is required for poleward chromosome movement during mitosis in Drosophila embryos. *Nat. Cell Biol.* 2:922-930.

Silva, K.A., J. Dong, Y. Dong, Y. Dong, N. Schor, D.J. Tweardy, L. Zhang, and W.E. Mitch. 2015. Inhibition of STAT3 activation suppresses caspase-3 and the ubiquitin-proteasome system, leading to preservation of muscle mass in cancer cachexia. *J. Biol. Chem.* 290:11177-11187.

Song, I., J.H. Kim, K. Kim, H.M. Jin, B.U. Youn, and N. Kim. 2009. Regulatory mechanism of NFATc1 in RANKL-induced osteoclast activation. *FEBS Lett.* 583:2435-2440.

Stockmann, M., M. Meyer-Ohlendorf, K. Achberger, S. Putz, M. Demestre, H. Yin, C. Hendrich, L. Linta, J. Heinrich, C. Brunner, C. Proepper, G.F. Kuh, B. Baumann, T. Langer, B. Schwalenstocker, K.E. Braunstein, C. von Arnim, S. Schneuwly, T. Meyer, P.C. Wong, T.M. Boeckers, A.C. Ludolph, and S. Liebau. 2013. The dynactin p150 subunit: cell biology studies of sequence changes found in ALS/MND and Parkinsonian syndromes. *J. Neural Transm.* 120:785-798.

Stowers, L., D. Yelon, L.J. Berg, and J. Chant. 1995. Regulation of the polarization of T cells toward antigen-presenting cells by Ras-related

GTPase CDC42. *Proc. Natl. Acad. Sci. U. S. A.* 92:5027-5031.

Takahashi, N., S. Ejiri, S. Yanagisawa, and H. Ozawa. 2007. Regulation of osteoclast polarization. *Odontology*. 95:1-9.

Takayanagi, H. 2005. Mechanistic insight into osteoclast differentiation in osteoimmunology. *J. Mol. Med. (Berl.)*. 83:170-179.

Takayanagi, H. 2007. Osteoimmunology: shared mechanisms and crosstalk between the immune and bone systems. *Nat. Rev. Immunol.* 7:292-304.

Takayanagi, H., S. Kim, T. Koga, H. Nishina, M. Isshiki, H. Yoshida, A. Saiura, M. Isobe, T. Yokochi, J. Inoue, E.F. Wagner, T.W. Mak, T. Kodama, and T. Taniguchi. 2002. Induction and activation of the transcription factor NFATc1 (NFAT2) integrate RANKL signaling in terminal differentiation of osteoclasts. *Dev. Cell*. 3:889-901.

Teitelbaum, S.L. 2000. Bone resorption by osteoclasts. *Science*. 289:1504-1508.

Thomas, S.M., and J.S. Brugge. 1997. Cellular functions regulated by Src family kinases. *Annu. Rev. Cell Dev. Biol.* 13:513-609.

Tsakiridis, T., C. Taha, S. Grinstein, and A. Klip. 1996. Insulin activates a p21-activated kinase in muscle cells via phosphatidylinositol 3-kinase. *J. Biol. Chem.* 271:19664-19667.

Vaira, S., M. Alhawagri, I. Anwisye, H. Kitaura, R. Faccio, and D.V. Novack. 2008. RelA/p65 promotes osteoclast differentiation by blocking a

RANKL-induced apoptotic JNK pathway in mice. *J. Clin. Invest.* 118:2088-2097.

Valetti, C., D.M. Wetzel, M. Schrader, M.J. Hasbani, S.R. Gill, T.E. Kreis, and T.A. Schroer. 1999. Role of dynactin in endocytic traffic: effects of dynamitin overexpression and colocalization with CLIP-170. *Mol. Biol. Cell*. 10:4107-4120.

Vallee, R.B., J.C. Williams, D. Varma, and L.E. Barnhart. 2004. Dynein: An ancient motor protein involved in multiple modes of transport. *J. Neurobiol.* 58:189-200.

Varma, D., P. Monzo, S.A. Stehman, and R.B. Vallee. 2008. Direct role of dynein motor in stable kinetochore-microtubule attachment, orientation, and alignment. *J. Cell Biol.* 182:1045-1054.

Vaughan, K.T., and R.B. Vallee. 1995. Cytoplasmic dynein binds dynactin through a direct interaction between the intermediate chains and p150Glued. *J. Cell Biol.* 131:1507-1516.

Wang, Y., D. Lebowitz, C. Sun, H. Thang, M.D. Grynpas, and M. Glogauer. 2008. Identifying the relative contributions of Rac1 and Rac2 to osteoclastogenesis. *J. Bone Miner. Res.* 23:260-270.

Warner, S.J., H. Yashiro, and G.D. Longmore. 2010. The Cdc42/Par6/aPKC polarity complex regulates apoptosis-induced compensatory proliferation

in epithelia. *Curr. Biol.* 20:677-686.

Waterman-Storer, C.M., S. Karki, and E.L. Holzbaur. 1995. The p150Glued component of the dynactin complex binds to both microtubules and the actin-related protein centractin (Arp-1). *Proc. Natl. Acad. Sci. U. S. A.* 92:1634-1638.

Waterman-Storer, C.M., S.B. Karki, S.A. Kuznetsov, J.S. Tabb, D.G. Weiss, G.M. Langford, and E.L. Holzbaur. 1997. The interaction between cytoplasmic dynein and dynactin is required for fast axonal transport. *Proc. Natl. Acad. Sci. U. S. A.* 94:12180-12185.

Wu, X., F. Quondamatteo, T. Lefever, A. Czuchra, H. Meyer, A. Chrostek, R. Paus, L. Langbein, and C. Brakebusch. 2006. Cdc42 controls progenitor cell differentiation and beta-catenin turnover in skin. *Genes Dev.* 20:571-585.

Yamauchi, J., Y. Miyamoto, H. Kokubu, H. Nishii, M. Okamoto, Y. Sugawara, A. Hirasawa, G. Tsujimoto, and H. Itoh. 2002. Endothelin suppresses cell migration via the JNK signaling pathway in a manner dependent upon Src kinase, Rac1, and Cdc42. *FEBS Lett.* 527:284-288.

Yue, L., S. Lu, J. Garces, T. Jin, and J. Li. 2000. Protein kinase C-regulated dynamitin-macrophage-enriched myristoylated alanine-rice C kinase substrate interaction is involved in macrophage cell spreading. *J. Biol.*

Chem. 275:23948-23956.

Zhang, Z., T. Welte, N. Troiano, S.E. Maher, X.Y. Fu, and A.L. Bothwell. 2005. Osteoporosis with increased osteoclastogenesis in hematopoietic cell-specific STAT3-deficient mice. *Biochem. Biophys. Res. Commun.* 328:800-807.

국문초록

파골세포 분화에 대한 dynactin1의 역할

서울대학교 대학원 세포및발생생물학 전공

(지도교수: 김 홍 희)

이 용 덕

골 항상성은 뼈를 형성하는 조골세포와 뼈를 흡수하는 파골세포의 활성에 의해 조절된다. 조골세포와 파골세포 기능의 불균형은 골다공증, 류마티스 관절염과 같은 골 질환을 유발한다. 파골세포 분화는 조혈모 유래 전구 세포로 부터 M-CSF와 RANKL에 의해 유도된다. 미세소관 모터인 dynein과 어댑터 dynactin은 소낭 운반, 유사분열방추의 형성, 세포질 분열 등의 다양한 세포내 현상에 관여한다. Dynein의 활성을 촉진한다는 의미에서 그 이름이 유래된 dynactin은 dynein의 어댑터 역할을 하며 11개의 서로 다른 개별 단백질로 구성된 1 mDa에 이르는 거대한 복합체이다. Dynein/Dynactin의 결합은

세포질에서의 그 복합체의 활성화에 필요하다. Dynactin의 결합은 dynein의 진행성을 증가시키고, dynein을 세포내 특정 위치로 표적 시키는 것을 돕는다. Dynactin1 (DCTN1)은 다양한 진핵생물들에서 흔하게 발현되며, dynactin 복합체 내에서 중추적인 역할을 하는 가장 큰 구성 단백질이다. DCTN1은 미세소관과 dynein에 동시에 결합하여 dynein의 진행성을 조절한다. DCTN1의 G59S 유전자 변이는 미세소관과의 결합기능을 상실케하여 다양한 신경퇴행성질환을 발생시킨다.

본 논문에서는 DCTN1의 파골세포 분화에서의 역할을 연구하였다. DCTN1의 knockdown은 MAPK phosphorylation과 NFATc1/c-Fos의 발현을 저해함으로써 파골세포 분화의 감소를 야기 하였다. 더욱이, DCTN1의 결손은 Cdc42와 PAK2의 활성에 영향을 미치고, actin-ring 형성을 저해 시켰다. DCTN1이 knockdown된 골수 유래 대식세포에 지속적인 활성을 띠는 Cdc42를 과발현 시켰을 때는, 파골세포 분화가 회복 되었다. NFATc1/c-Fos의 발현 역시 회복 되었다. 흥미롭게도, DCTN1 과발현을 유도 하였을 때에도 파골세포 분화가 감소 됨을 확인 하였다. 이러한 결과로 미루어 볼 때 DCTN1 발현을 적절한 수준으로 유지 하는게 정상적인 파골세포 분

화에 중요한 것으로 보인다. 또한, 쥐의 두개골에 RANKL을 적신 콜라겐 스폰지를 이식하는 동물 실험을 통하여 DCTN1 knockdown이 실제로 파골세포 분화와 골 흡수를 억제시킬 수 있다는 사실을 확인하였다. 결론적으로, 본 논문에서는 DCTN1이 파골세포 분화에 있어서 중요한 인자임을 확인 하였다.

주요어 : 파골세포 분화, dynactin1, NFATc1, c-Fos, Cdc42, PAK2

학 번 : 2009-23600